Investigating Impacts of Local Circulation on Coastal Ozone Pollution in the New York Metropolitan Area: Evidence from Multi-year Observations

Huiying Luo[1,2] and Cheng-Hsuan Lu[1,3]

[1]Atmospheric Sciences Research Center, University at Albany, State University of New York, Albany, NY 12226, USA
[2]Now at Colorado State University, Fort Collins, CO 80523, USA
[3]Joint Center for Satellite Data Assimilation, University Corporation for Atmospheric Research, Boulder, CO 80301, USA

Correspondence author: Huiying Luo (luohuiying0313@gmail.com)

Key Points:

1. K-means clustering is applied to group local circulation and temperature diurnal cycles during the summertime of 2017-2019.

2. Hot summer day ozone would drop 9-10 ppb when sea breeze is delayed and intercepted by the dominant westerlies in ozone hot spots.

3. Early morning meridional wind direction would control sea breeze onset type and modulate ozone exceedances during extreme conditions.

Abstract

Elevated surface ozone levels are often detected in the New York (NY) metropolitan area during summertime. Moreover, surface ozone in this region exhibits sharp spatial gradients and distinctive diurnal cycles under the influence of complex boundary layer circulation induced by the intricate coastal geometry. This study examines how surface ozone is impacted by local circulation spatially and temporally under different temperature scenarios (all summer days, hot summer days, and extreme heat days) with the help of cluster-based meteorological conditions during the summertime of 2017-2019. The most polluted days are found to be highly associated with hot sea breeze days with weak background flow. When sea breeze development in the New York Bight is delayed and its penetration north is intercepted by the dominant westerlies during hot summer days, daily maximum 8-hour average ozone (DMA8) in some ozone hot spots of New York City (NYC) and the south shore of Connecticut (CT) would typically drop 9-10 ppb under comparable temperature levels. The average regional decrease of DMA8 for NYC and coastal CT is 6.7 and 8.3 ppb, respectively. Furthermore, we conclude that a change in early morning meridional wind direction is the most critical meteorological characteristic in controlling sea breeze onset type and helping modulate ozone exceedances in the region during extreme heat days when ozone exceedances are expected to be very common. The conclusion is further demonstrated with two case studies during the Long Island Sound Tropospheric Ozone Study (LISTOS) 2018 field campaign.

Plain Language Summary

The New York metropolitan area is classified as a moderate 8-hour ozone nonattainment area by the U.S. Environmental Protection Agency. Moreover, surface ozone in this region exhibits sharp horizontal and vertical gradients and distinctive diurnal cycles under the influence of complex boundary layer circulation. This study examined three summers of meteorological (wind and temperature) and chemical (ozone and its precursors of nitrogen oxides and formaldehyde) observations to investigate the impacts of local circulation on coastal ozone pollution in the area, with a focus on hot summer days when high concentrations of ozone are more likely. With the projected extreme heat in the region increasing in intensity and duration throughout the 21st

century, meteorological characteristics most critical in modulating ozone exceedances in ozone hot spots during extreme heat days are identified and analyzed with case studies during the Long Island Sound Tropospheric Ozone Study (LISTOS) field campaign.

1 Introduction

The New York (NY) metropolitan area, including New York City (NYC), Long Island (LI), the south shore of Connecticut (CT), and the northeast corner of New Jersey (NJ), is the most populous built-up area in the United States. Elevated surface ozone levels are often detected in the region during summertime thanks to favorable meteorological conditions such as high temperature and abundant local anthropogenic and natural ozone precursor emissions of nitrogen oxides (NOx, consisting of NO and NO_2) and volatile organic compounds (VOCs). The region is classified as a moderate 8-hour ozone nonattainment area (area that has a design value of 81 up to but not including 93 ppb, US EPA, 2018) with the Ozone National Ambient Air Quality Standards (NAAQS) level at 70 ppb.

Moreover, surface ozone in the NY metropolitan area exhibits sharp horizontal and vertical gradients and distinctive diurnal cycles under the influence of complex boundary layer circulation, such as the commonly detected Atlantic sea breeze (sea breeze developed along the south coast of LI) and sound breeze from Long Island Sound (LIS) induced by the intricate coastal geometry throughout the region (Couillard et al., 2021; Han et al., 2022; McCabe & Freedman, 2023; Novak & Colle, 2006; Zhang et al., 2020). Other large water bodies in the region, such as the Hudson River, Upper Bay, Lower Bay, and Newark Bay, also have the potential to influence local circulation due to land/water temperature contrast. In addition, the large-scale urbanization in the region alters the local circulation with its excessive heat flux and increased surface roughness. Urban heat island (UHI) generated by the heat contrast between the urban center and surrounding area produces convergence flow into the urban center. The convergent flow would accelerate the sea breeze front towards the city center (Freitas et al., 2007; Hu et al., 2022). However, sea breeze front penetration over the city center would likely be more difficult and can be stalled for a few hours (Freitas at al., 2007; Hu et al., 2022) due to the convergent flow and urban frictional retardation and would be slower overall than that over less-urbanized surrounding areas (Ferdiansyah et al., 2020; Han et al., 2022). These interactions have been found to strongly affect urban air pollution (Bornstein & Thompson, 1981; Han et al., 2022; Khiem et al., 2010; Ulpiani, 2021).

Impacts of local circulation on surface ozone have been studied across many coastal regions worldwide, especially near or around urban centers where high ozone remains a threat to public health. Many of them are case studies using observations (Banta et al., 2005; Couillard et al., 2021; Han et al., 2022; Zhang et al., 2022), numerical modeling (Ding et al., 2004; Torres-Vazquez et al., 2022) or both (Caicedo et al., 2019; Finardi et al., 2018; Liu et al., 2022). It has been found that large-scale flow direction, sea breeze characteristics, and vertical mixing all play essential roles in controlling ozone horizontal and vertical distribution. Sea breeze characteristics include location/penetration, timing, depth, and intensity/strength. Specifically, for the NY region, Zhang et al. (2022) found that the north shore of LI experienced the highest ozone during stagnant or sea breeze days, while the south shore high ozone always involved westerly or southwesterly flow; Torres-Vazquez et al. (2022) found that ozone over CT is especially sensitive to local wind features. Despite numerous case studies examining the influence of local circulation on the coastal ozone problem in the NY metropolitan area, particularly during the Long Island Sound Tropospheric Ozone Study (LISTOS) 2018 field campaign (e.g., Han et al., 2022; Torres-Vazquez et al., 2022; Zhang et al., 2022), a comprehensive investigation over an extended period is warranted to better summarize local conditions and serve as a reference for future case studies.

Long-term studies routinely employ group-based comparisons across diverse scenarios, such as sea breeze days and non-sea breeze days. Ngan & Byun (2011) and Li et al. (2020) examined the ozone levels at various circulation conditions in Houston with gridded analysis products and in-situ and remote sensing observations, respectively. The highest ozone is found to be associated with sea breeze days in the Houston region (Li et al., 2020). Papanastasiou and Melas (2009) studied the difference in observed ozone diurnal cycles during sea breeze versus non-sea breeze days in the Volos area of Greece. They concluded that the presence of sea breeze will increase ozone concentrations, and the increase is more pronounced during cold months. Oh et al. (2006) compared the observed diurnal variations in ozone and NO_2 during early and late sea breeze onset days in the Busan metropolitan area in Korea and explored the mechanisms with case studies using numerical modeling. It is found that offshore synoptic flows delay the onset of sea breeze and help preserve urban emission above the sea from early morning, which will be recirculated back with sea breeze, leading to a significant enhancement of maximum ozone by a factor of 1.5 compared with early sea breeze onset condition.

However, these group-based comparison studies only focused on specific aspects of local circulation and overlooked the importance of temperature to local ozone levels, despite the well-established strong correlation between surface ozone levels and temperature (Coates et al., 2016; Olszyna et al., 1997; Porter & Heald, 2019). Higher temperatures often indicate clear sky conditions with higher levels of solar radiation reaching the lower atmosphere. Together, they favor higher surface ozone concentration by 1) accelerating photochemical reaction rates and 2) boosting VOCs and NOx emissions from both natural and anthropogenic sources through various processes, such as accelerated biogenic emission of VOCs and increased NOx emissions from higher energy demand for air conditioning (Coates et al., 2016; Guenther et al., 1995; Porter & Heald, 2019). In addition, higher temperature facilitates the growth of a deeper planetary boundary layer (PBL) due to increased convection driven by surface heating. However, the impacts of PBL height on surface ozone are often coupled with influences from other physical and chemical factors, including the absolute height of PBL and ozone vertical profile (Haman et al., 2014; Zhang et al., 2023). The overall effect of PBL height on surface ozone is less certain. In general, the highest surface ozone most likely occurs when PBL height is moderate (between 1-2 km for Beijing) and decreases as PBL becomes higher (dilution) or lower (decreased photochemistry because of the availability of sunlight) (Zhang et al., 2023).

With the addition of temperature as a contributing factor, this study adapted the k-means clustering technique used in Li et al. (2020) to cluster NYC wind conditions and diurnal temperature profiles. It comprehensively investigated the impacts of local circulation on coastal ozone pollution in the area using three summers of meteorological and chemical observations. Specific questions we will answer in this study are:

1. What is the general relationship between surface ozone and meteorological conditions in the region during summertime?
2. What are the temporal and spatial characteristics of ozone during hot summer days, when elevated ozone levels are more prevalent, and how does local circulation contribute to these patterns?
3. Can local circulation help modulate ozone exceedances during extreme heat events, and if so, how?

The contents are organized as follows. Details of data and methodologies are described in Section 2. Section 3.1 addresses the first question by presenting the cluster results and examining the overall impact of local circulation and temperature scenarios on daily maximum 8-hour average ozone (DMA8) spatial distribution in the New York metropolitan area during the summertime of 2017-2019. Then, Section 3.2 focuses on hot summer days, during which ozone levels are more elevated and harmful to human health and other living beings, and summarizes how background wind conditions and sea breeze impact ozone diurnal cycles and spatial distributions, answering the second question. Lastly, critical meteorological characteristics that can help modulate ozone exceedances during extreme hot sea breeze days in ozone hot spots of NYC and coastal CT are identified and illustrated with representative case studies during LISTOS in Section 3.3 (the third question). A comprehensive table detailing all related meteorological characteristics and ozone levels during hot sea breeze days is also included to serve as a reference for future case studies.

2 Data and Methods

2.1 Data

Multi-platform meteorological and chemical observations during the summertime (June-July-August, JJA) of 2017-2019 were collected to help answer the three scientific questions above. All surface and lidar observations with temporal resolution higher than an hour have been averaged to hourly data for consistency and more straightforward interpretation. The hour for all hourly data indicates the end of the averaging window in EST (UTC - 05:00, EST is used throughout this study), e.g., 11:01 to 12:00 is averaged for the 12:00 condition for data measured at 1 min frequency.

Hourly surface ozone observations and hourly NOx and meteorological observations at available co-located sites were directly obtained from the pre-generated annual files from the US Environmental Protection Agency (EPA) Air Quality System website (AQS, https://aqs.epa.gov/aqsweb/airdata/download_files.html). Since they are reported at the sample starting time, all AQS observations are shifted one hour to be consistent. Ozone, NOx, and NO_2 observations used in this study are measured by either a Federal Reference Method (FRM) or a Federal Equivalent Method (FEM) as defined in the Code of Federal Regulations for Ambient

Air Monitoring Reference and Equivalent Methods (https://www.ecfr.gov/current/title-40/chapter-I/subchapter-C/part-53). Locations of these air quality monitoring sites are marked with red triangles in Figure 1. Specifically, site 360810124 at Queens, NY, and 090019003 at Westport, CT, both with NO_2 observations, are annotated in red on the map. Both sites have been utilized to study how local circulation modulates ozone exceedances during extreme hot sea breeze days in the highly polluted NYC and coastal CT regions.

Additional hourly surface meteorological observations were assembled from the New York State Mesonet (NYSM, https://www2.nysmesonet.org/) (Brotzge et al., 2020), the Automated Surface Observing Systems (ASOS, https://www.ncei.noaa.gov/products/land-based-station), and the National Data Buoy Center (NDBC, https://www.ndbc.noaa.gov/). Their locations, including those of those AQS sites with meteorological observations, are shown with black dots in Figure 1. NYSM performs both automated and manual quality control to flag out erroneous data. Pre-generated hourly NYSM data was obtained directly by data request at the official website. One-minute observations from ASOS were downloaded and averaged to the end of the hour. Buoy data is reported at various temporal resolutions from several minutes to one hour at the end-of-acquisition time. The same averaging was conducted for those observations with higher temporal resolutions. Specifically, hourly data is reported at two buoy sites (44025 and 44064) used to represent air temperature in the New York Bight at hh:50 and shifted ten minutes to (hh+1):00.

Among these, the newly established NYSM delivers quality-controlled hourly average meteorological fields with extraordinary temporal data coverage. For example, site QUEE at Queens, NY, experienced only two missing days for temperature and one missing day for surface wind during the three summers we studied. Thus, eight NYSM surface sites (thick gray circles in Figure 1), located in NYC and LI, in addition to those two buoy sites, 44025 and 44065 (thick gray circles in the ocean in Figure 1), both located south of LI, were adopted to calculate regional meteorological conditions over land and sea, respectively. Among these eight NYSM surface sites, Queens, NY (QUEE) in NYC and Wantagh, NY (WANT) in LI were used to cluster local weather conditions and annotated in black on the map.

NYSM wind Doppler lidar (WDL, Leosphere scanning Doppler Windcube 100S) collects data using the Doppler Beam Swinging (DBS) scan mode, which consists of five scans in four cardinal directions (north, east, south, and west) and nadir with a cycle of 20 seconds (Shrestha et al., 2021). These scans are then combined to reconstruct the three-dimensional wind profiles (zonal wind u, meridional wind v, and vertical wind w) from 100 to 7000 m above ground level, with a vertical resolution of 25-50 m and a temporal resolution of 1 s. In this study, we utilized hourly averaged horizontal wind profiles from 100 m to 2000 m at 100 m intervals above the surface at Wantagh, NY, on the south shore of LI to estimate the depth of sea breeze developed from the Atlantic Ocean. Details of sea breeze feature identification are described in Section 2.3. The Doppler lidar site is located less than 0.5 km away from NYSM surface site WANT and hereafter referred as WANT as well.

Weather map composites from National Oceanic and Atmospheric Administration (NOAA) High-Resolution Rapid Refresh (HRRR, https://registry.opendata.aws/noaa-hrrr-pds/) hourly reanalysis fields, with a horizontal resolution of 3 km, were used to characterize large-scale weather conditions for local circulation clusters of interest during hot summer days. In addition, we employed the gradient in HRRR hourly surface wind fields to locate the sea breeze fronts in the case studies in Section 3.3.

We also obtained Version R1 vertical column HCHO and NO_2 densities below the aircraft (resolution of 0.01°) retrieved from The Geostationary Coastal and Air Pollution Events (GEO-CAPE) Airborne Simulator (GCAS) and Geostationary Trace gas and Aerosol Sensor Optimization (GeoTASO) onboard National Aeronautics and Space Administration (NASA) aircrafts during the LISTOS 2018 field campaign (https://www-air.larc.nasa.gov/cgi-bin/ArcView/listos). These observations were used to investigate the spatial distribution of HCHO and NO_2 and derive the ozone chemical regime during morning and noon times in the case studies (Section 3.3) under different background circulation and sea breeze onset conditions.

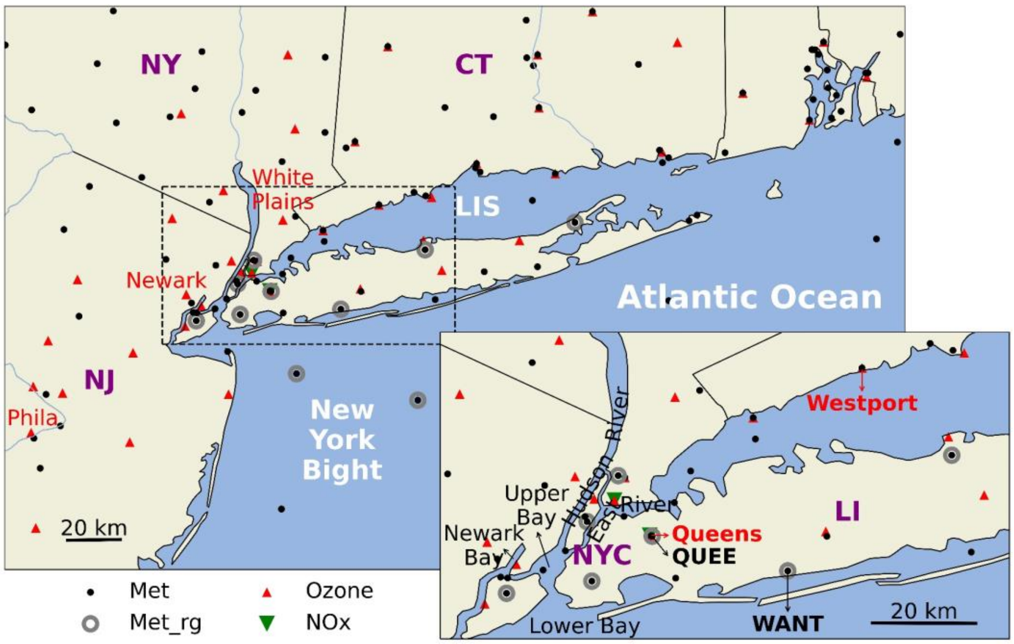

Figure 1. Coastal geometry of the NY metropolitan area and locations of observation stations. Dash black rectangle in the main figure indicates the location of the NYC insert. Meteorological sites (*Met*) from NYSM, ASOS, AQS, and NDBC are marked with black dots. Thick gray outlines highlight eight NYSM sites over land and two NDBC sites over the ocean used for regional quantitative analysis (*Met_rg*) in Section 3. AQS ozone sites (*Ozone*) are represented by red triangles. Among them, two sites in the NYC region with NOx observations (*NOx*) used in Section 3.2 are highlighted by green reverse triangles. Locations referenced in the study are also marked on the map, with "Phila" representing Philadelphia.

2.2 Clustering of local weather conditions

In order to study the impacts of local circulation on ozone spatial and temporal distribution, it is necessary to limit the influence of temperature given the high correlation between surface ozone level and temperature. K-means clustering is an effective and efficient technique to separate features of interest into distinctive groups (Li et al., 2020; Macqueen, 1967; Xu et al., 2021). It separates samples into clusters by minimizing the *inertia* or within-cluster sum-of-squares:

$$\sum_{i=1}^{I}\sum_{j=1}^{J} w_{ij}\,\left\|x_i-\mu_j\right\|^2 \qquad (1)$$

in which x_i is the input feature vector of sample *i*, with *i* from 1 to *I*; μ_j is the centroids of cluster *j* (mean of samples in cluster *j*). *j* is from 1 to a user pre-defined cluster number *J*. w_{ij} = 1 when sample x_i belongs to cluster *j*; otherwise, w_{ij} = 0.

Major limitations of k-means clustering are that the number of clusters needs to be preselected and the convergent results are dependent on initial centroids. We addressed these with the help of the KMeans function in scikit-learn (Pedregosa et al., 2011), a free machine learning library for the Python programming language. Further details will be discussed below when clustering temperature and wind conditions at QUEE. QUEE is selected because 1) as part of the newly established NYSM, this site delivers quality controlled hourly average meteorological observations with extraordinary temporal data coverage; 2) it is "collocated" with an active AQS site reporting both ozone and NOx observations; 3) observations from AQS and NYSM at this site are representative in both physical and chemical conditions around the NYC where high ozone episodes occur frequently.

For temperature, 24 hourly mean temperatures at QUEE from 00:00 to 23:00 were directly used as input features. We preselected the number of clusters at three, and the initial cluster centroids sampling method was set to be based on an empirical probability distribution to speed up convergence and guarantee the *inertia* converging to a global minimum (Pedregosa et al., 2011). The resultant clusters are named *Hot*, *Moderate*, and *Cool* days based on their diurnal temperature profile, and their statistics will be discussed in Section 3.1.

We also applied k-means clustering to categorize local circulation conditions represented by six features derived from diurnal time series of hourly surface wind conditions at QUEE. The features were adapted from Li et al. (2020), in which they clustered the wind conditions in the Houston and San Antonio regions separately based on seven characteristics derived from local wind observations. The first four features of morning and afternoon wind components remain similar: morning zonal (u, first feature) and meridional (v, second feature) winds were averaged during the early morning of 04:00-06:00 and afternoon u (third feature) and v (fourth feature) winds were averaged during the early afternoon of 14:00-16:00, respectively. As there is no apparent land breeze development during the early morning of sea breeze days in NY metropolitan area (McCabe & Freedman, 2023), days with strong southerly wind (southerly throughout the day) and sea breeze days (calm in the early morning and southerly during sea breeze hours in the region) would not be distinguishable using the original last three features in Li et al. (2020) as they all focus on the temporal variation of wind directions throughout the day (results for QUEE shown in Figure S1). Thus, we replaced these last three features with two new ones designed to separate southerly from sea breeze days: average early morning (04:00-06:00) wind speed (fifth feature) and the ratio of morning and afternoon mean wind speed (sixth feature) by dividing the average early morning wind speed by the average afternoon (14:00-16:00) wind speed. All features were normalized across the three summers before the cluster analysis since k-means clustering groups the features of interest by minimizing the Euclidean distance to the centroids. Normalization allows each feature to have the same weight during the process. The number of clusters was tested between 3 and 6, and four clusters yielded the best wind condition separations (small *inertia* and reasonable wind clusters by visual inspection of the clustering results for all summer days) were adopted. The same initialization approach was set to speed up the convergence and find the global minimum as used in the temperature clustering. The four resultant clusters of *Sea Breeze* (*SB*), *Oscillation* (*O*), *Southerly* (*S*), *and Westerly* (*W*) days, all named based on their wind directions and speeds throughout the day, will be discussed in detail in Section 3.1.

2.3 Sea breeze feature identification

Critical features of sea breeze impacting coastal ozone levels, as identified in previous case studies, are estimated based on NYSM surface and wind lidar observations at the coastal site of WANT during *Hot SB* days. Figure 2 demonstrates the identification of those sea breeze features on Aug. 5, 2018, including sea breeze depth (*SB_Depth, Figure 2a*), sea breeze onset v wind instant change (*SB_dV*, *Figure 2b*), sea breeze onset time (*SB_OnT, Figure 2b*), and sea breeze strength (*SB_Str*, *Figure 2b*). *SB_dV* is defined as the maximum hourly gradient (change in the next hour from the current hour) in 10 m v wind during 07:00-16:00. *SB_OnT* (10:00 in the example) is the hour following the time when *SB_dV* occurs. *SB_Str* is estimated to be the average 10 m v difference between 3 hours after onset time (11:00-13:00 in the example) and early morning of 04:00-06:00. *SB_Depth* is the height above ground at which the correlation of v wind with 10 m v wind drops below 0.5 starting from 100 m to 2000 m. Six hours (starting from the hour when *SB_dV* occurs, 09:00-14:00 in the example), instead of the whole sea breeze period, were utilized in the estimation to avoid the ambiguity in deciding the sea breeze cessation time and the impact of low-level jet developed in the later hours during some of the sea breeze days. Note that the detected *SB_OnT* and *SB_Str* might not be as reliable when the wind speed of the Atlantic sea breeze increases gradually on some of the days with relatively stronger background onshore flow in the early morning. In addition, stronger upper-level flow and lidar data availability during some of the *Hot SB* days might challenge the quality of the identified *SB_Depth*.

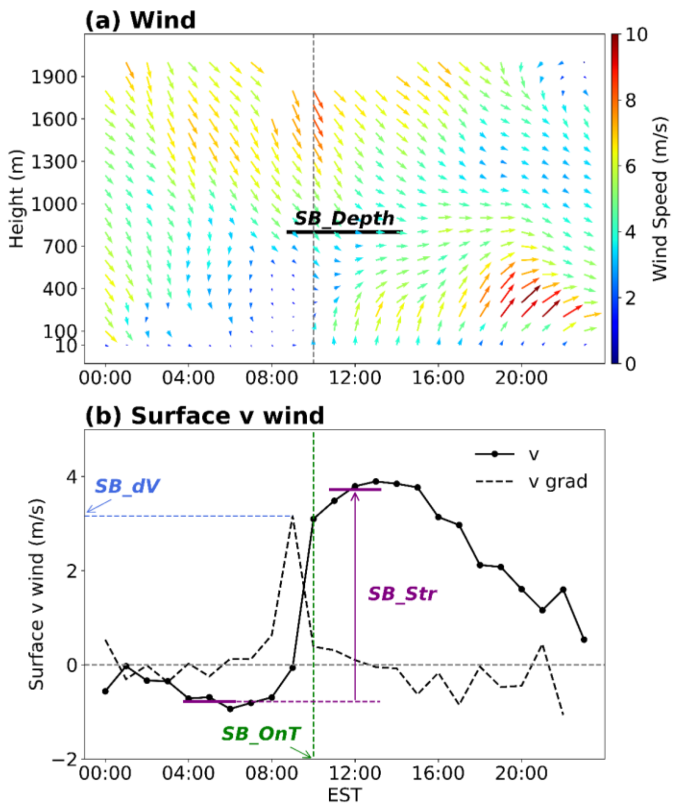

Figure 2. Sea breeze feature identification at WANT on Aug. 5, 2018: (a) 10 m surface wind and horizontal wind profiles at 100s meters above ground level with identified sea breeze depth (*SB_Depth*) marked with a thick black line; (b) time series of 10 m v wind (negative values indicate wind from the north and positive values indicate wind from the south; the same convention applies throughout this study) and its gradient with sea breeze strength (*SB_Str*), onset time (*SB_OnT*), and onset v wind instant change (*SB_dV*) illustrated.

Sea breeze front locations in two case studies in Section 3.3 were estimated based on hourly HRRR surface wind reanalysis fields by calculating the wind gradient *Grad* in x and y directions as follows:

$$Grad[x,y] = \sqrt{(u[x,y]-u[x+1,y])^2+(v[x,y]-v[x+1,y])^2} + \sqrt{(u[x,y]-u[x,y+1])^2+(v[x,y]-v[x,y+1])^2} \quad (2)$$

in which *x* and *y* represent the grid cell location; *u* and *v* are the 10 m wind components. The longitude *lonxy* and latitude *latxy* of the grid cell for *Grad* is calculated by:

$$lonxy[x,y] = \frac{lon[x,y]+lon[x,y+1]}{2} \quad (3)$$

$$latxy[x,y] = \frac{lat[x,y]+lat[x+1,y]}{2} \quad (4)$$

in which *lon* and *lat* are the longitude and latitude of the original HRRR grid cell. Higher values of *Grad* indicate higher contrast in wind speed and directions. Lines formed by connected higher *Grad* values would signal the location of possible fronts, including sea breeze fronts.

3 Results and Discussions

3.1 Meteorological clustering results and summertime all-weather ozone distribution

The clustered diurnal cycles of temperature at QUEE are shown in Figure 3. During the three summers (median temperatures are described below), 70 days are clustered as *Hot* days with maximum temperature around 30.7°C at 14:00 and minimum temperature around 24.2°C at 05:00, 132 days are clustered as *Moderate* days with maximum temperature around 26.8°C at 14:00 and minimum temperature around 21.3°C at 05:00, and 72 days are clustered as *Cool* days with maximum temperature around 22.2°C at 15:00 and minimum temperature around 17.2°C at 05:00. The clean separation among the interquartile ranges of the three temperature clusters indicates the effectiveness of the k-means clustering.

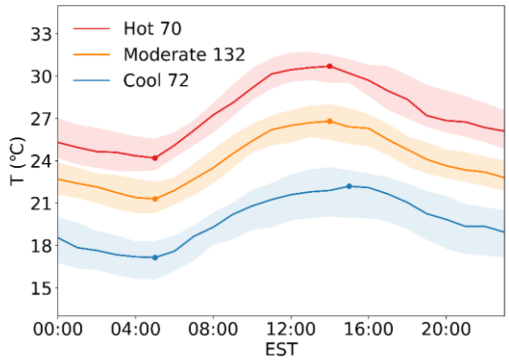

Figure 3. Diurnal cycles of three temperature clusters of *Hot*, *Moderate*, and *Cool* days at QUEE. Median temperatures (solid lines) with their maximum and minimum (marked in dots) and interquartile range (light-colored shades) of each cluster are shown. The number of days in each cluster is shown in the legend.

Figures 4a and b display the average hourly wind vectors and early morning and afternoon wind roses for four wind clusters of *Sea Breeze* (*SB*), *Oscillation* (*O*), *Southerly* (*S*), and *Westerly* (*W*) at QUEE. In total, 113 *SB* days have been identified with light wind in the early morning and much stronger southerly wind from the Atlantic Ocean in the afternoon. There is no apparent land breeze developed during nighttime, agreeing to what is found in McCabe & Freedman (2023). The weaker sound breeze developed from LIS towards LI and CT, as identified in previous studies (Han et al., 2022; Novak & Colle, 2006), normally does not penetrate into NYC and are thus not reflected in the wind conditions at QUEE. Similar to the clustering results in Li et al., 2020, an *Oscillation* cluster has been identified. It consists of 69 days impacted by strong large-scale wind flow with slowly clockwise-rotating wind. The *Southerly* cluster represents 36 days with consistent southerly wind throughout the day. Its daytime southerly wind tends to be strengthened by sea breeze due to the land-sea temperature contrast, and its wind speed peaks early around noontime compared with 15:00 in the *SB* cluster with light synoptic flow in the region. Note that sea breeze, any wind that blows from a large body of water toward or onto a landmass, as a physical phenomenon might happen under many synoptic-scale wind conditions, such as in the *Southerly* cluster; the italicized cluster *Sea Breeze* (*SB*) only refers to the days in that cluster with relatively calm background wind fields. Lastly, 57 *Westerly* days have been found to have constant westerly wind blowing into NYC. The westerlies are intensified by a northwest component during the afternoon.

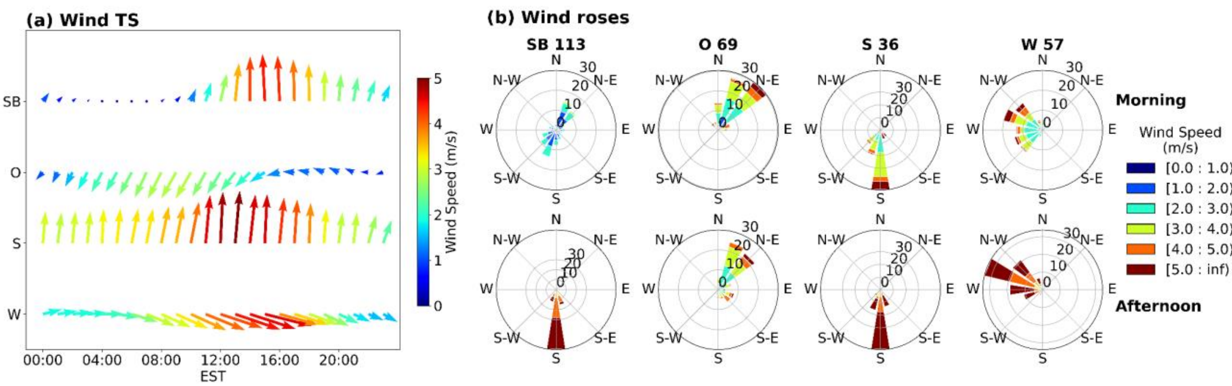

Figure 4. Wind clusters at QUEE. (a) diurnal cycles of mean wind for four wind clusters of *Sea Breeze* (*SB*), *Oscillation* (*O*), *Southerly* (*S*), and *Westerly* (*W*); (b) early morning (04:00-06:00, top panels) and afternoon (14:00-16:00, bottom panels) wind roses for each wind cluster. The number of days in each cluster is shown in (b).

With temperature and wind diurnal cycles clustered, we first confirmed the effectiveness of those clustering by checking the consistency of their statistics across ten combined clusters (Table 1, two clusters with less than six days are excluded from the analysis due to the scarcity of such weather conditions). As expected, daytime temperature is generally consistent during *Hot* (28.0-30.0°C), *Moderate* (24.9-25.7°C), and *Cool* (19.9-21.6°C) days across different wind conditions; morning wind speed and wind speed ratio statistics are also consistent at different temperature levels. For example, *SB* days have the lowest morning wind speeds at 1.7-1.8 m/s and ratios of morning and afternoon wind speeds of 0.4 for all three temperature clusters.

Summertime all-weather ozone distribution for all combined meteorological clusters is shown in Figure 5 and summarized in Table 1. It is clear that temperature and local circulation have distinctive impacts on daily ozone levels in the region. As noted previously, higher temperature facilitates higher ozone production in general. A specific wind pattern exhibits consistent effects on the spatial distribution of ozone, regardless of temperature levels (also see Figure S2 for DMA8 spatial anomaly with the cluster average removed). Specifically, *SB* days favor high ozone levels along the Philadelphia-NYC-LIS corridor (dashed gray line in Figure 5a), especially for *Hot* and *Moderate* days (Figures 5a and d, S2a and d). During *S* days, the region is occupied by moist and modest marine air brought in by the steady southerly flow. Due to the similarity in wind directions compared with *SB* days, similar high ozone locations are observed on *S* days, with an expansion of high ozone levels into the CT inland region (Figures 5b and f, S2b and f). The region south of the Philadelphia-NYC-LIS corridor experiences higher ozone levels during *W* days at all temperature levels (Figures 5c, g, and j; S2c, g, and j). *O* days tend to be accompanied by lower temperature levels (*Moderate* and *Cool*) and observe the lowest ozone levels during *Cool* summer days with an average DMA8 of 33.4 ppb (Figures 5e and i; Table 1).

It is clear that the most polluted days are closely associated with *Hot SB* days (DMA8 at 60.4 ppb and 8.7 sites with ozone exceedances per day on average) with weak large-scale flow in the early morning, followed by *Hot W* days (DMA8 at 53.5 ppb and 2.4 sites with ozone exceedances per day). *Hot* summer days during which ozone exceedances (DMA8 > 70 ppb) are expected to happen much more frequently will be further studied in the following sections.

Table 1. Summary of summertime meteorological clusters and regional ozone characteristics. SD stands for Standard Deviation. Daytime temperature is averaged from 07:00 to 17:00 EST. Morning wind speed and wind speed ratio refer to the fifth and sixth feature, respectively, as discussed in Section 2.2. Ozone exceedance (DMA8 > 70 ppb) occurrences count all sites, as shown in Figure 5, during all days in each cluster. Ozone exceedance occurrences (/day) are then calculated by dividing that by the number of days in the cluster.

	Temperature cluster	***Hot***			***Moderate***				***Cool***		
	Wind cluster	***SB***	***S***	***W***	***SB***	***O***	***S***	***W***	***SB***	***O***	***W***
Cluster statistics at QUEE	Number of days	37	7	22	54	27	25	26	22	37	9
	Daytime temperature mean (°C)	29.4	28.0	30.0	25.7	24.9	25.4	25.5	21.1	19.9	21.6
	Daytime temperature SD (°C)	1.2	1.3	1.9	1.3	1.6	1.1	1.4	1.7	2.5	1.5
	Morning wind speed mean (m/s)	1.8	3.0	2.6	1.7	2.5	3.9	3.3	1.7	3.3	3.3
	Morning wind speed SD (m/s)	0.4	0.5	0.8	0.5	0.9	1.3	1.1	0.6	1.0	1.0
	Wind speed ratio mean	0.4	0.7	0.6	0.4	0.9	0.8	0.7	0.4	1.1	0.6
	Wind speed ratio SD	0.1	0.4	0.2	0.1	0.3	0.3	0.2	0.1	0.4	0.2
Regional ozone	DMA8 spatial mean (ppb)	60.4	46.9	53.5	49.1	41.2	42.9	41.7	41.2	33.4	40.8
	DMA8 spatial SD (ppb)	5.5	5.0	6.0	3.1	4.0	2.8	3.8	2.3	1.6	2.9
	Ozone exceedance occurrences	323	9	52	69	2	32	7	0	0	0
	Ozone exceedance occurrences (/day)	8.7	1.3	2.4	1.3	0.1	1.3	0.3	0.0	0.0	0.0

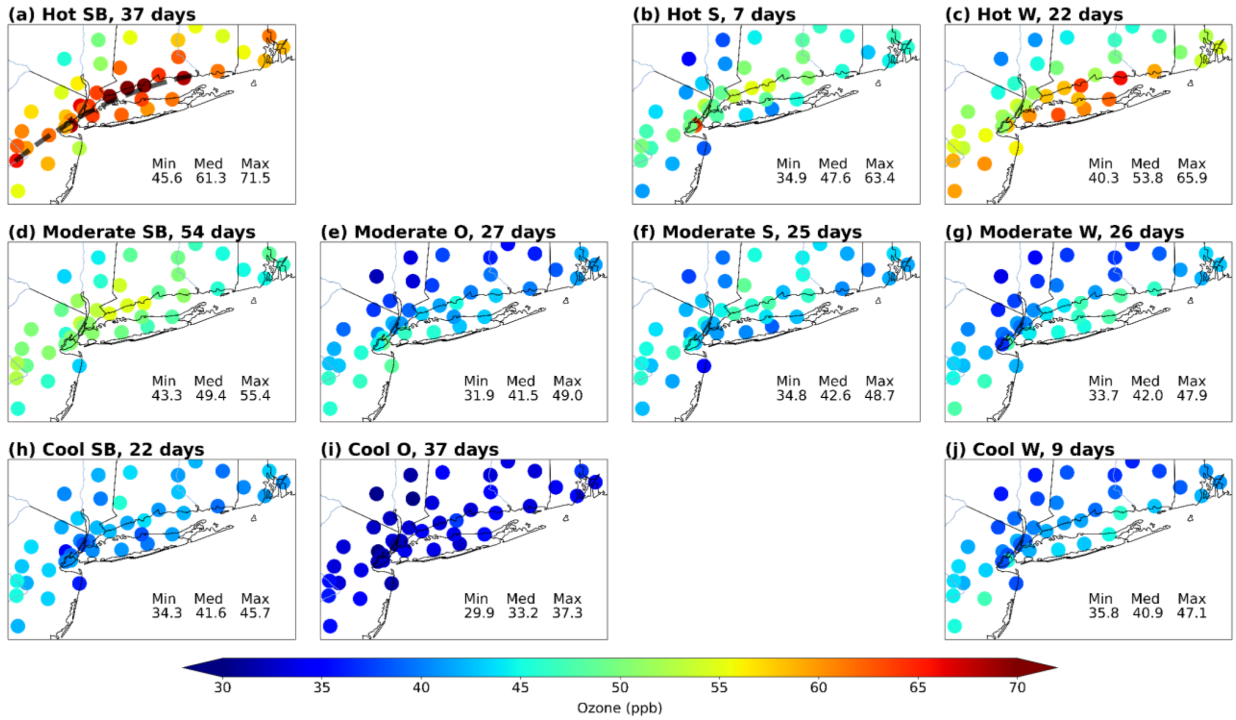

Figure 5. Average DMA8 for all meteorological clusters with at least six days during the summertime (JJA) of 2017-2019. The number of days in each cluster is marked on the map.

3.2 Impacts of local circulation on ozone during hot summer days

As sea breeze develops and penetrates NYC during both *Hot SB* and *S* days, we first examined whether sea breeze developed during *Hot W* days along south LI by looking at wind conditions at WANT. It turns out sea breeze develops along south LI during most *Hot W* days but fails to penetrate into NYC (QUEE) because of the dominant westerlies. Thus, *Hot W* days are further divided into two subsets according to the afternoon (13:00-16:00) mean v wind direction at WANT (Figure 6). Namely, they are *Hot W_w* and *Hot W_sb* days, with lowercase *w* and *sb* representing afternoon conditions at WANT. Five *W_w* days with persistent strong northwesterlies at WANT in the afternoon are detected among 22 *Hot W* days and will be ignored hereafter because of the limited number of days and their low ozone levels. Cluster *W_sb* consists of 17 *Hot W* days with delayed sea breeze onset (around 11:00 at the coastal site of WANT, as in Figure 6, compared with 09:00-10:00 at QUEE, a site further inland in NYC, as in

Figure 4a) and penetration of sea breeze inland to the northwest part of the study region (such as QUEE) intercepted by the dominant westerlies.

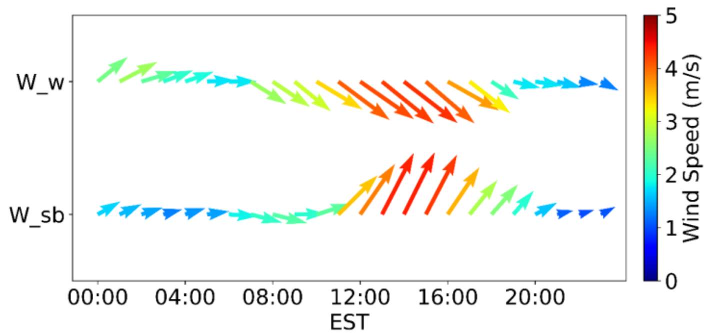

Figure 6. Diurnal cycles of mean 10 m wind at WANT during *Hot W* wind subsets of *W_w* (5 days) and *W_sb* (17 days). The lowercase *w* and *sb* in the subset names represent coastal wind conditions of westerly and sea breeze at WANT.

Weather maps based on composites of HRRR reanalysis fields of 850 hPa geopotential height and wind during *Hot* day clusters (*SB*, *W_sb*, and *S*) are shown in Figure 7. It should be noted that sea breeze developed from the Atlantic Ocean in all three clusters. However, the characteristics of the sea breeze vary in geographical extent, magnitude, and timing. The Bermuda High pressure system ("H" in Figure 7) sits near the Southeast Coast of the contiguous United States (CONUS) during summertime, generating light southwesterlies in the study region during *Hot SB* days (Figures 4a and 7a). When the low-pressure system in southeastern Canada ("L" in Figure 7) moves eastwards and pushes the north part of Bermuda High south during *Hot W_sb* days, westerly components of the local wind around the NY metropolitan area strengthen, delaying the sea breeze development near the coast and preventing its penetration further inland to the city center (Figures 4a, 6, and 7b). Strong southerly wind in the New York Bight and its coastal region is generated during *Hot S* days as the Bermuda High advances closer to the Northeast Coast of CONUS with its large-scale clockwise rotation (Figure 7c). The southerly wind strengthens during daytime as the Atlantic sea breeze develops (Figure

4a).

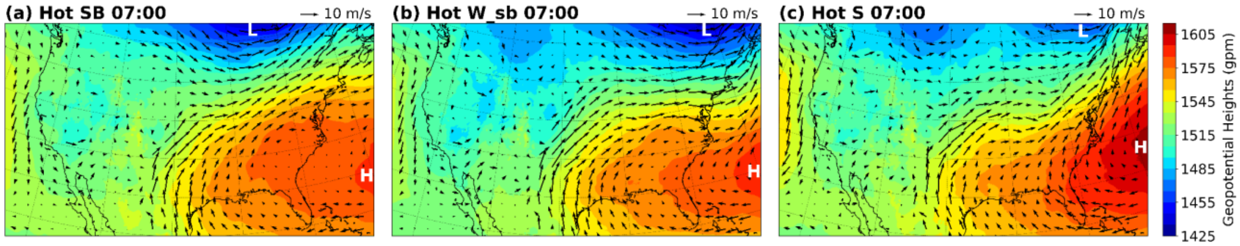

Figure 7. 850 hPa average weather conditions at 07:00 for *Hot* (a) *SB* (37 days), (b) *W_sb* (17 days), and (c) *S* (7 days) clusters. Wind speed and direction are represented by black vectors; colored contours indicate the 850 hPa geopotential heights in geopotential meters (gpm) with intervals of 10 gpm; relative locations of major high (H) and low (L) pressure systems impacting the NY metropolitan area are marked in white.

Similar to what is shown in Figure 5, Figures 8a-c displays the spatial distribution of average DMA8 for three *Hot* day clusters, with the modification of *W* to *W_sb* days. As expected, mean DMA8 on *W_sb* days (median value of 56.0 ppb) increased notably along LI and coastal CT compared with *Hot W* days (median value of 53.8 ppb) in Figure 5 after removing the *W_w* days. In addition, the probability of daily DMA8 exceeding the NAAQS level of 70 ppb (*Pex*) for each cluster is shown in Figures 8d-f. During *Hot SB* days, the three most polluted sites located in coastal Fairfield County (southwest CT) observed mean DMA8 higher than 70 ppb with corresponding *Pex* around 50%. Among them, mean DMA8 and *Pex* at Westport, CT, is 71.5 ppb and 43.2%, respectively. Slightly lower DMA8 and *Pex* are observed at other sites along the CT coastline and Queens, NY (mean DMA8 = 63.8 ppb, *Pex* = 40.5%). *Pex* for *W_sb* (median value of 5.9%) and *S* days (median value of 0.0%) and DMA8 for *S* days decreased dramatically compared with *SB* days (median value of 18.9%).

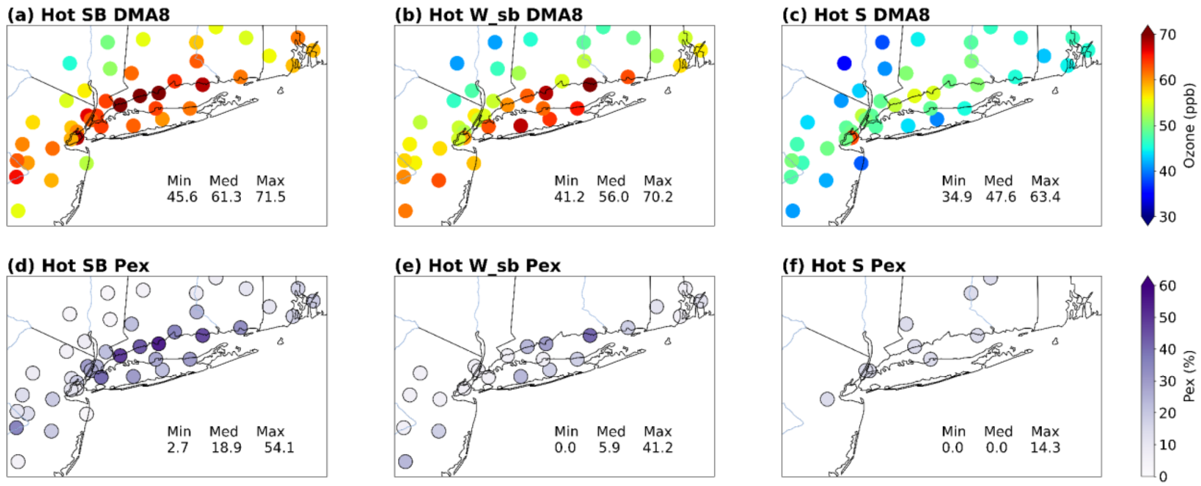

Figure 8. (a-c) DMA8 mean and (d-f) percentage of days with DMA8 exceeding NAAQS of 70 ppb (*Pex*, sites with no exceedance are not shown) on *Hot* (a, d) *SB*, (b, e) *W_sb*, and (c, f) *S* days. Note that sites with no ozone exceedance (*Pex* = 0.0) are not shown in (d-f) for clarity, but the minimum, median, and maximum statistics are calculated based on all sites.

To better understand the change in DMA8 levels for different local circulation clusters, we looked into the regional ozone, NOx (NYC only where observations are relatively abundant), and temperature diurnal cycles (Figure 9), with differences in DMA8 between most polluted *Hot SB* and *W_sb* days shown in Figure 9h. In addition, ozone tendency maps overlaid with local wind conditions are displayed in Figure 10. The three high ozone exceedance probability (high *Pex*) regions of NYC (squares in Figure 9h), CTcoastal (coastal region of western CT, triangles in Figure 9h), and LICTe (LI and coastal region of eastern CT, reverse triangles in Figure 9h) are selected and grouped manually based on their spatial proximity and similarity in the characteristics of their ozone diurnal cycles during *SB*, *W_sb*, and *S* days.

When sea breeze development in the New York Bight is delayed and its penetration into the NYC and shores of western LIS is intercepted by the dominant westerlies (*W_sb*) (Figures 10d-f), DMA8 in the hot spots around NYC and western CT would typically drop 9-10 ppb (Figure 9h) under comparable temperature levels (Figures 9b, e, and g, Table 2) compared with *Hot SB* days. The average regional decrease of DMA8 for NYC and CTcoastal regions is 6.7 and 8.3 ppb, respectively (Table 2). Higher levels of local NOx emission are accumulated in the NYC region during the morning time of *SB* days due to the continuous NOx emission from industrial sources and stagnant nighttime conditions. NOx levels begin to drop after 07:00 as the photochemical production of ozone is initiated after sunrise (Figures 9a and c). Compared with *SB* days, the rate of ozone increasing in the early morning during *W_sb* days is much lower, and ozone level plateaus much earlier, around 11:00, at lower levels in NYC as strong westerly carry the local pollutants downwind (Figures 9a and 10d-e). In CTcoastal, ozone increases fast in the morning time and decreases in the afternoon at a similar rate during both *SB* and *W_sb* days (Figure 9d); the 9-10 ppb difference in DMA8 in CTcoastal stems from the additional fueling during *SB* days around noon time. While ozone build-up time during *W_sb* days in LICTe becomes hours longer compared with *SB* days because of the stationary sea breeze/westerly front in the region (Figures 10d-f), comparable or even higher DMA8 levels are observed, especially in southeastern LI (Figure 9h). Zhang et al. (2022) also found that the high ozone cases at the Heckscher State Park (south shore of LI) always involve the westerlies and southwesterly flow.

Lowest ozone levels are observed during *Southerly* days for all three regions because of the presence of marine air (warmer during nighttime and colder during daytime) throughout the day brought in by the steady southerly flow (Table 2; Figures 9 and 10g-i). The largest difference in ozone levels is observed in LICTe due to its proximity to the northerly moving and relatively cleaner marine air from the Atlantic Ocean. Ozone starts to drop as early as 12:00 at some sites in NYC and LICTe, especially for the highly polluted site at Queens, NY (Figures 9a, f, and Figure 10h). CTcoastal experiences the least improvement in air quality during *S* days, likely due to the transported polluted air trapped in the shallow boundary layer above LIS (Torres-Vazquez et al., 2022). The secondary peak of ozone in the late afternoon, around 19:00-20:00, during *Hot S* days might be brought to all three regions by the return flow of the sea breeze circulation, with southerly flow dying down in the meantime.

Table 2. *Hot* summer day average condition for NYC, CTcoastal, and LICTe. Daytime temperature is averaged from 07:00 to 17:00 EST.

	NYC			**CTcoastal**			**LICTe**		
	SB	***W_sb***	***S***	***SB***	***W_sb***	***S***	***SB***	***W_sb***	***S***
Daytime Temperature (°C)	30.0	30.2	28.6	28.3	28.8	27.2	27.8	28.4	27.2
DMA8 (ppb)	63.7	57.0	49.1	67.6	59.3	51.7	62.5	65.6	45.3

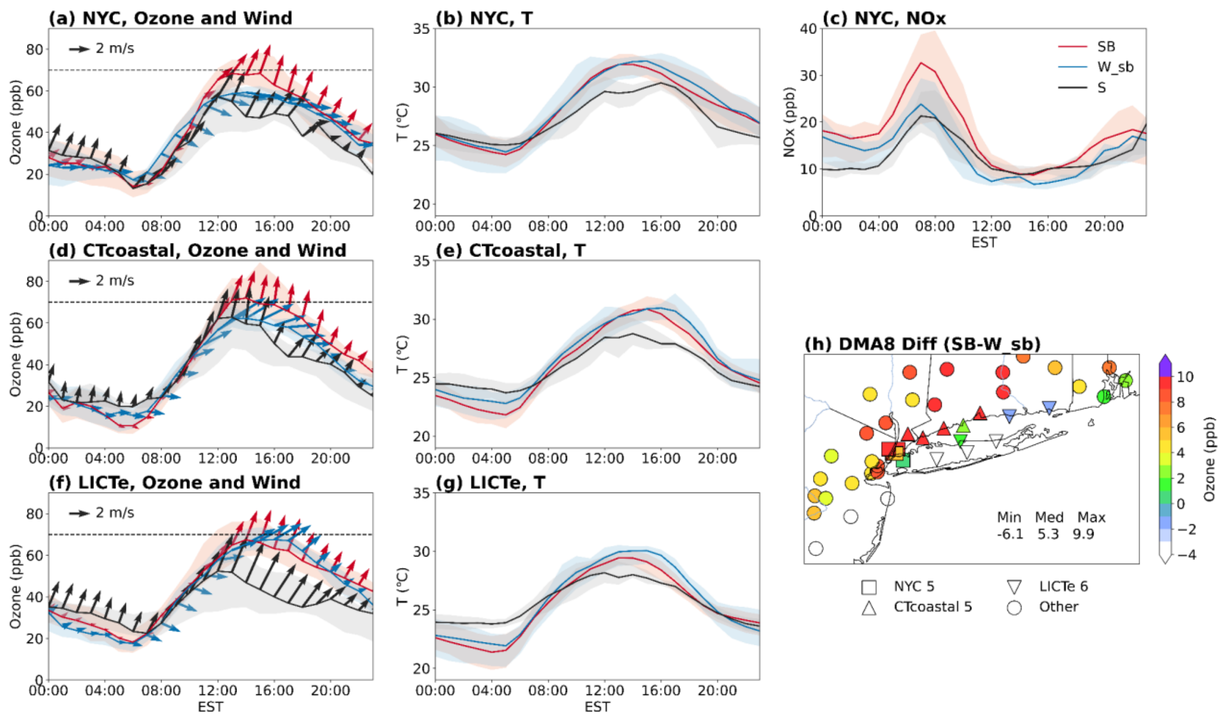

Figure 9. Regional ozone, surface wind, temperature, and NO_x (NYC only) diurnal cycles during *Hot SB*, *W_sb*, and *S* days for (a-c) NYC (square in h), (d-e) CTcoastal (triangle in h), and (f-g) LICTe (reverse triangle in h), with stations used for the regional composite marked in (h) the *Hot SB* and *W_sb* DMA8 difference map with number of sites in each region shown in the legend. Solid lines represent average conditions (median condition for ozone) with interquartile ranges shaded in the same colors.

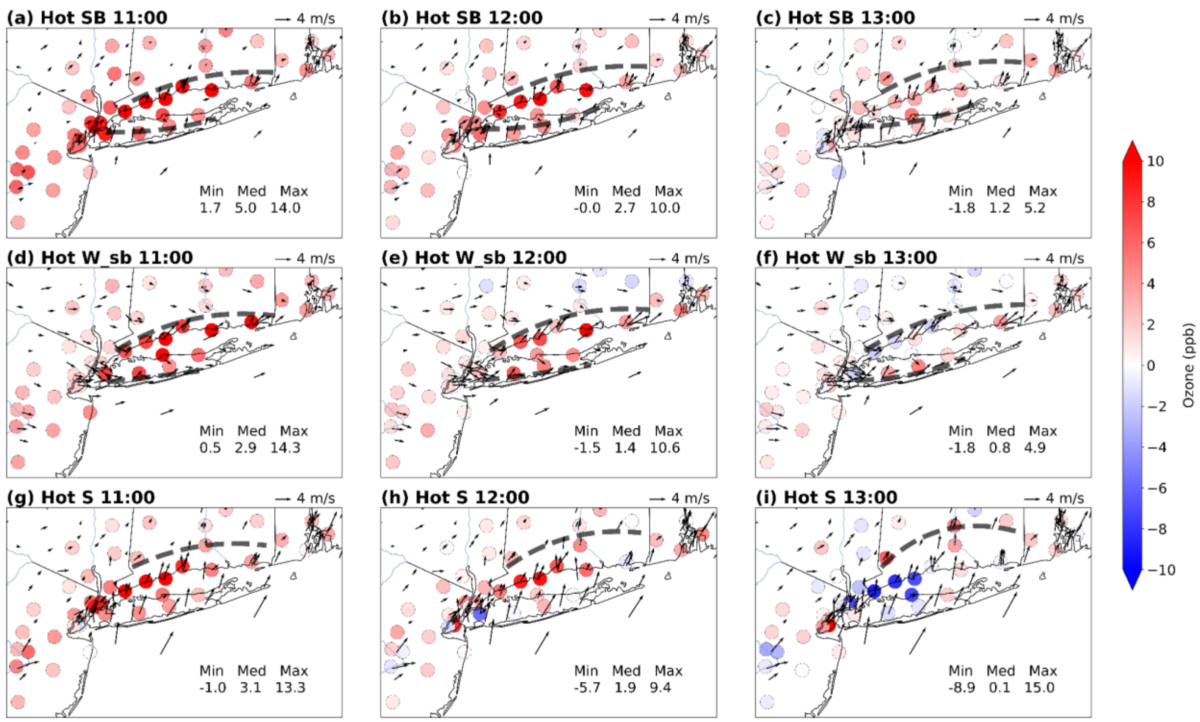

Figure 10. Average ozone tendency, calculated by subtracting ozone at the current hour from ozone at the next hour, during *Hot* (a-c) *SB*, (d-f) *W_sb*, and (g-i) *S* days from 11:00 to 13:00 (left to right). Sea breeze front locations are manually marked with dashed gray lines (the weaker sound breeze towards LI is not marked with limited surface observations) based on the observed surface wind (magenta wind vectors).

3.3 How local circulation modulate ozone exceedances in extreme heat

With the projected extreme heat in NYC increasing in intensity and duration throughout the 21st century (RCP4.5 and RCP8.5) (Ortiz et al., 2019), ozone levels are expected to rise under current emission conditions. This section examines whether local circulation can modulate ozone exceedances in extreme high heat by analyzing the meteorological characteristics for ozone exceedance and non-exceedance days at the most polluted NYC (Queens, NY as example) and CTcoastal (Westport, CT as example) regions (Figures 8a and d) during *hot SB* days. In addition to four sea breeze features identified at WANT, as discussed in Section 2.3, we also included the following meteorological features:

- Sea breeze arrival time at the ozone monitoring site (*SB_ArrT*). The identification process of *SB_ArrT* is the same as *SB_OnT*, except for using surface v wind at or near the ozone monitoring site (NYSM site QUEE for Queens, NY, and co-located wind observation at AQS site 090019003 for Westport, CT).

- Regional average early morning v wind during 04:00-06:00 (*V_am*) at eight NYSM surface sites highlighted with thick black outlines in Figure 1.
- Regional average early morning u wind during 04:00-06:00 (*U_am*) at the same eight sites.
- Regional average daytime mean temperature during 07:00-17:00 (*T*) at the same eight sites.
- Regional average daytime temperature difference from the sea during 07:00-17:00 (*dT*). Sea temperature is calculated at two NDBC sites highlighted with thick blue outlines in Figure 1.

To select those days with extreme high heat and minimize the ozone dependence on temperature, we limited our analysis to 16 *Hot SB* days with regional daytime temperature (*T*) higher than 29°C, defined as extreme heat/hot days in this study. The threshold of 29°C is manually picked to effectively de-correlate DMA8 at Queens, NY, and *T* based on their scatter plot (Figure S3). Note that ozone observations at Westport, CT are missing during 2 out of the 16 days. As expected, ozone exceedances (DMA8 > 70 ppb) happened during the majority of the extreme hot days at both locations (11 out of 14 days for Westport, CT, and 11 out of 16 days for Queens, NY). Among the 14 days with ozone observations at Westport, CT, 7 days witnessed ozone exceedances at both locations. Only 1 (Aug. 5, 2018, Sunday) out of the 14 days did not experience ozone exceedance for both locations, most likely due to the limited availability of NOx emissions during the weekend (Figure S4). DMA8 that day for Westport and Queens are at 60.6 ppb and 66.4 ppb, respectively. Days with different ozone exceedances at the two locations are Jun. 30, 2018, and Jun. 28, 2019, for ozone exceedances at Queens but not Westport； and Jul. 19, 2017, Aug. 28, 2018, Jul. 28, 2019, and Jul. 30, 2019, for ozone exceedances at Westport but not Queens.

Figure 11 presents the ozone levels and meteorological features (detailed in Section 2.3 and the beginning of this section) during ozone exceedance and non-exceedance days at Queens, NY, and Westport, CT. Panels from left to right are organized by units and magnitudes of the variables. Even though Queens is located closer to major emission sources, its DMA8 and hourly peak ozone level (*O_3_max*) are significantly lower than those of Westport during ozone exceedance days. In addition, both DMA8 and *O_3_max* at Westport differ significantly during ozone exceedance and non-exceedance days. Both phenomena signify the importance of transport in modulating ozone exceedances in the region (Figures 11a and g). During extreme hot days, the median *T* difference between ozone exceedance and non-exceedance days is very minimal at 0.1 and 0.2°C at Queens and Westport, respectively (Figures 11e and k). The same is true for the depth of sea breeze (*SB_Depth*) (Figures 11d and j). Likely due to the removal of colder days, no significant difference is found in median sea breeze onset (*SB_OnT*) and arrival time (*SB_ArrT*) (Figures 11b and h). Sea breeze tends to develop early in coastal areas during extreme hot days because of the higher contrast in land/sea temperature and penetrated into NYC two to three hours later. Due to the impact of the LIS sound breeze, there is large uncertainty in the estimation of sea breeze arrival time *SB_ArrT* at Westport, CT.

Theoretically, a higher contrast in land/sea temperature (*dT*) observed during ozone exceedance days (around 0.4°C higher than non-exceedance days for both locations, Figures 11f and l) would favor a stronger sea breeze onset. However, the sea breeze strength (*SB_Str*) and onset type (higher *SB_dV* for abrupt sea breeze onset and lower for gradual sea breeze onset) depend more on the early morning wind conditions in the region (Figures 11c and i). During extreme *hot SB* days with relatively stagnant early morning conditions, a relatively stronger southerly wind component (higher *V_am* around 1m/s) in the early morning will favor gradual (lower *SB_dV*) weak (lower *SB_Str*) sea breeze development (Figure 11c). When coupled with slightly stronger morning westerlies (higher *U_am*), these gradual weak sea breeze days would typically yield lower chances of ozone exceedances in NYC (Figures 11a and c). On the contrary, a relatively stronger northerly wind component (higher negative *V_am* around -1 m/s) in the early morning will likely lead to abrupt (higher *SB_dV*) strong (higher *SB_Str*) sea breeze onset (Figure 11i). This finding is consistent with the previous lake breeze study in Salt Lake Valley, in which they concluded that opposing flow would contribute to stronger lake breeze front (Blaylock et al., 2017). In this case, the south shore of CT would see a lower possibility of ozone exceedances, especially when morning westerly flow is weaker (lower *U_am*) (Figures 11g and i). In the following, we will illustrate how these differences in local circulation conditions, stemming from the subtle early morning meridional wind (*V_am*) contrast, modulate ozone exceedances in these two regions using two case studies during the LISTOS field campaign.

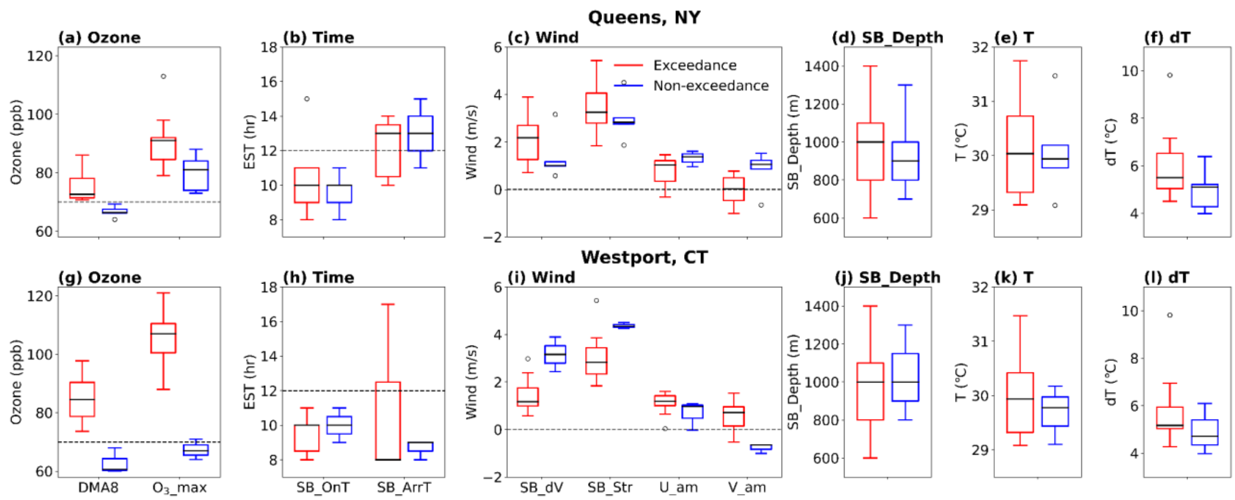

Figure 11. Ozone levels and meteorological features during ozone exceedance days (DMA8 > 70 ppb, red) and non-exceedance days (DMA8 ≤ 70 ppb, blue) for Queens, NY (top panels) and Westport, CT (bottom panels) under extreme high heat (T > 29 °C). Panels from left to right are for: (a, g) DMA8 and O_3*_max* with NAAQS level of 70 ppb marked with dash line; (b, h) *SB_OnT* and *SB_ArrT* with 12:00 marked with dash line; (c, i) wind conditions of *SB_dV*, *SB_Str*, *U_am*, and *V_am* with 0 m/s marked with dash line; (d, j) *SB_Depth*; (e, k) T; and (f, l) dT. Boxplots show interquartile range (IQR) with the median value in black; the whiskers spread to the farthest point if within 1.5 times the IQR from the box; data points outside the whisker limits are shown as black open circles.

Case 1: Abrupt strong sea breeze onset

Jun. 30, 2018, is on a Saturday with regional daytime mean temperature (T) of 30.2°C and northerly background wind in the early morning (*V_am* = -1.0 m/s). Higher ozone levels around noon time are confined within the NYC area (Figure 12b). Specifically, DMA8 at Queens (ozone exceedance) and Westport (non-exceedance) are at 72.6 and 60.0 ppb, respectively. The case study is demonstrated using monitored surface wind and temperature (Figure 12a), ozone and NO_2 (Figure 12d), and spatial distribution of monitored ozone (Figures 12b and c) and ozone tendency (Figures 12e and f) overlaid with surface wind gradient based on HRRR. In addition, the vertical column density (VCD) of NO_2 and HCHO, as well as the chemical regime estimated by their ratio, are shown in Figure 13 to illustrate chemical conditions during the early morning and afternoon.

In the early morning, around 05:00, the ozone level at Queens dipped below 5 ppb, indicating strong NO titration (O_3 removal by NO) around NYC because of continuous NO emission from industrial sources and stagnant conditions during the nighttime, which facilitated the NOx accumulation around the source region (Figures 12a and d). This type of extensive urban-scale “hole” with extremely low surface ozone has been widely reported in previous studies such as Zhang et al. (2004). After sunrise and before the sea breeze arrival, the early morning northwesterly wind strengthened in NYC (Figure 12d), transporting NO_2 in the southeastern direction (Figure 13a). LIS sound breeze towards coastal CT developed at 10:00 as the land surface temperature rose. It remained a southerly flow throughout the day, making ozone over coastal CT sensitive to ozone and its precursors over the LIS. The sea breeze fully developed at WANT around 10:00 and arrived at QUEE only one hour later (Figure 12a). Apart from the sea breeze from the Atlantic Ocean, complex local circulation systems around the NYC region developed and sustained into the afternoon due to the urban/suburban and land/water temperature contrast (Figures 12e and f). These systems include the divergent sound breeze along LIS, river breeze along the Hudson River, and bay breeze at the coast of Upper Bay, Lower Bay, and Newark Bay, and convergence tendency (UHI) around urban centers of NYC and Newark. After the sea breeze penetrated into the NYC area, its further north movement was hindered by these strong local circulation systems. NO_2 transported southeast of NYC was recircuited back with the sea breeze from the Atlantic Ocean and accumulated around the city center (Figure 13d) because of the stationary convergent flow generated from the systems described above, facilitating long hours of ozone buildup around the city center, especially north of NYC at White Plains (Figures 12f). Figure 12d highlights the long hours of high ozone observed at Queens.

Although the high ozone levels tend to be confined around NYC in abrupt sea breeze cases, the complex circulation systems do not always fully develop because of the difference in synoptic wind conditions, in addition to urban/suburban and land/water temperature contrast (Figure S4 and S5). However, sound breeze towards CT and LI is consistently detected in all three cases (Figures 12, S4, and S5). Without the complex circulation system as on Jun. 30, 2018, sea breeze typically arrives at Queens two hours after its onset at WANT with light northwesterlies in the early morning. Ozone at Queens, sitting in between two fronts moving towards each other (front parallel to the CT coastline exserted by the background northwesterlies and sea breeze front from the Atlantic Ocean), rises faster before sea breeze from the Atlantic Ocean arrives and drops immediately after the sea breeze front passes by in two other cases shown in Figure S4 and S5.

Ozone levels in CTcoastal, however, are more NOx-sensitive. In days with light northwesterly flow in the early morning, NOx from NYC is not effectively transported to LIS and coastal CT, making the regional ozone production fall in the NOx-limited regime throughout the day (Figures 13c and f). Balanced between transport and chemical reactions, ozone at Westport plateaued early from 11:00 likely due to the limited NOx (Figures 12 and 13c, f), till night time at around 20:00 (similar in two other cases in Figure S4 and S5).

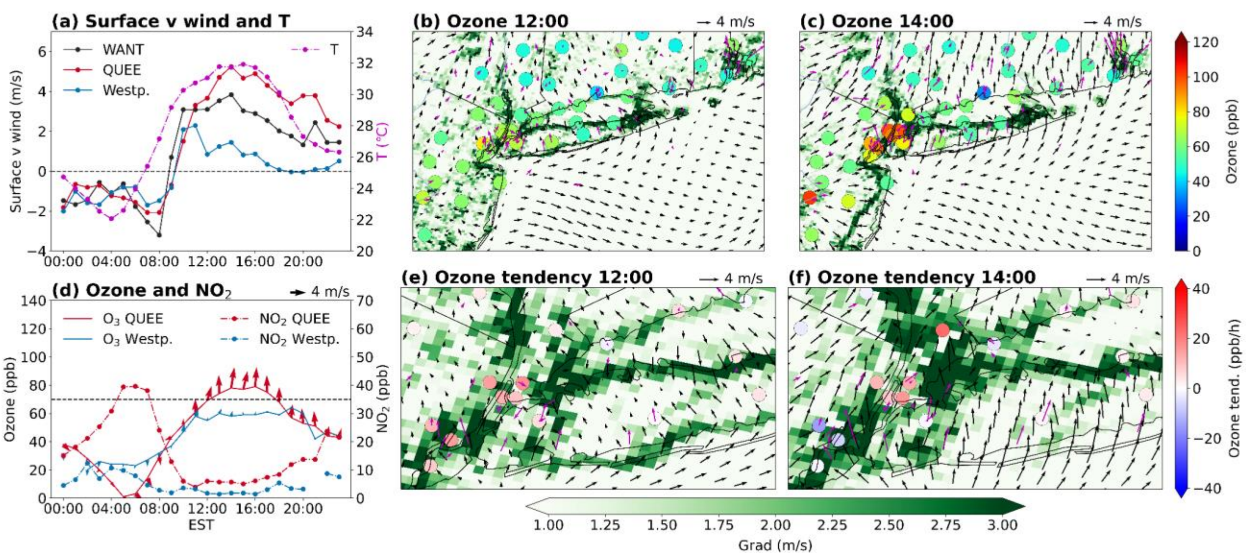

Figure 12. Abrupt strong sea breeze onset case on Jun. 30, 2018: (a) 10 m v wind at WANT, QUEE, and Westport with diurnal mean 2m temperature in the NYC-LI region; (b-c) Ozone distribution (filled color circles) and surface wind vectors from observations (magenta) and HRRR reanalysis wind field (black vectors) at 12:00 (c) and 14:00 (d) with front locations (green shade) signified by surface wind gradient (*Grad*, see Section 2.3); (d) Ozone and NO_2 time series at Queens and Westport with NAAQS level of 70 ppb marked with dash line; (e-f) hourly ozone tendency (filled color circles) and local wind conditions (same as in b) around NYC at 12:00 (e) and 14:00 (f).

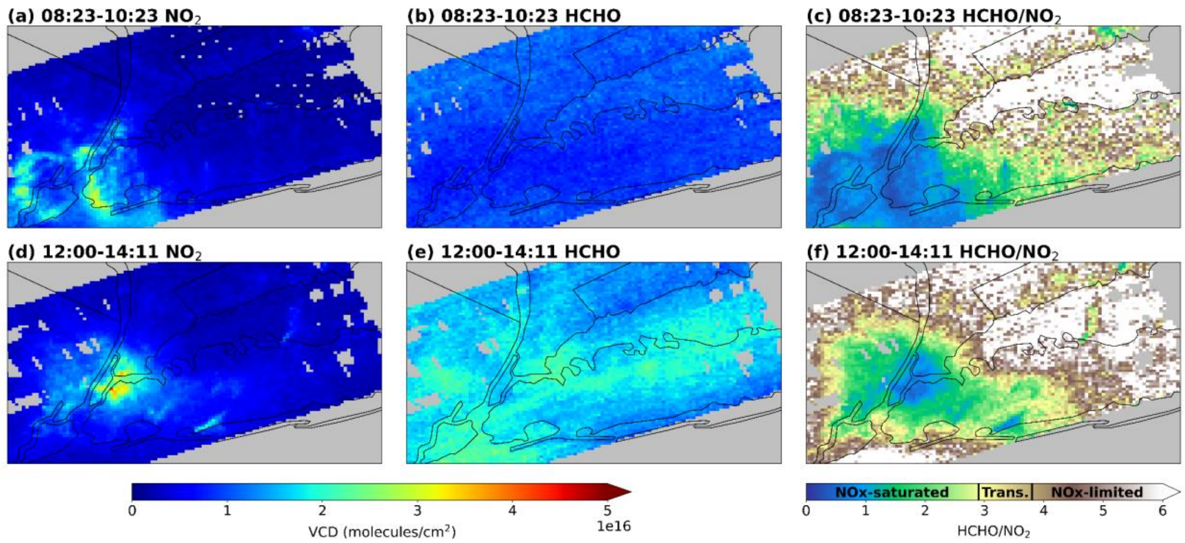

Figure 13. Abrupt strong sea breeze onset case on Jun. 30, 2018: vertical column density (VCD) of (a,d) NO_2, (b,e) HCHO, and (c,f) chemical regime estimated by their ratio ($HCHO/NO_2$) below aircraft (data from GeoTASO) in the morning (a-c) and early afternoon (d-f) around NYC. The ozone chemical regime in (c) and (f) follows the method used in Tao et al. (2022) with thresholds estimated in Jin et al. (2020) (transitional regime when $HCHO/NO_2$ ratios range from 2.9 to 3.8, with ratios below this range for the NOx-saturated/VOC-limited scenario and above for the NOx-limited/VOC-saturated scenario).

Case 2: Gradual weak sea breeze onset

Aug. 28, 2018, is on a Tuesday with regional daytime mean temperature (*T*) of 31.5°C and southerly background wind in the early morning (*V_am* = 0.9 m/s). High ozone levels around noon time are observed along the CT coastline (Figure 14c). Specifically, DMA8 at Queens (ozone non-exceedance) and Westport (exceedance) are at 66.3 and 84.5 ppb, respectively. Noticeable higher levels of HCHO are observed in the morning and afternoon across the region (Figures 15b and e), likely due to the acceleration of biogenic VOC emissions driven by the higher temperature throughout the day. The higher temperature would also yield more active photochemistry. The higher energy demand and weekday/weekend effect (the Jun. 30 case is on Saturday, and the Aug. 28 case is on Tuesday) might also increase the NOx loading on this day.

With southwesterly background flow starting before midnight, a large load of NO_2 emitted from sources around NYC was diluted downwind along LIS, making these regions NOx-saturated in the morning (Figures 15a and c). NO titration is observed at Westport with very minimal levels of ozone and high levels of NO_2 before sunrise (Figure 14c). Gradual (Figure 14a) and weak (lower wind gradient as seen in Figures 15b, c, e, and f) sea breeze front from the Atlantic Ocean developed early and carried higher concentrations of NOx and HCHO northward with it, favoring the extreme high ozone production in coastal CT, LI, and LIS around early afternoon (Figures 14f and 15d, e). In the meantime, the LIS sound breeze towards coastal CT developed and remained a southerly flow throughout the day as in the abrupt strong sea breeze case. The resultant peak hour ozone at Westport is well above 100 ppb. Likely coupled with the incoming polluted air confined in the shallow marine boundary layer above LIS with very active ozone production, the hourly increase of ozone at Westport could reach up to more than 40 ppb (reported on Jul. 30, 2019, Figure S6) as marine air progressed north from LIS (Figure S6d). Finally, the sea breeze front arrived at Westport in the late afternoon (around 17:00), and the decreasing of ozone slowed down with its progression towards coastal CT (Figures 14, S6, and S7).

Likely due to the limited availability of NOx, which is diluted away by the consistent stronger southwesterly flow (Figures 12a and 14a) and shorter period of weaker convergent flow around NYC (Figures 12e and 14e) compared with abrupt strong sea breeze days, ozone at Queens was not able to achieve high peaks and quickly decreased as the sea breeze front passed by (Figure 14d). With a stronger westerly component in the background wind, the ozone level might start to drop even before the sea breeze front arrives (Figure S7).

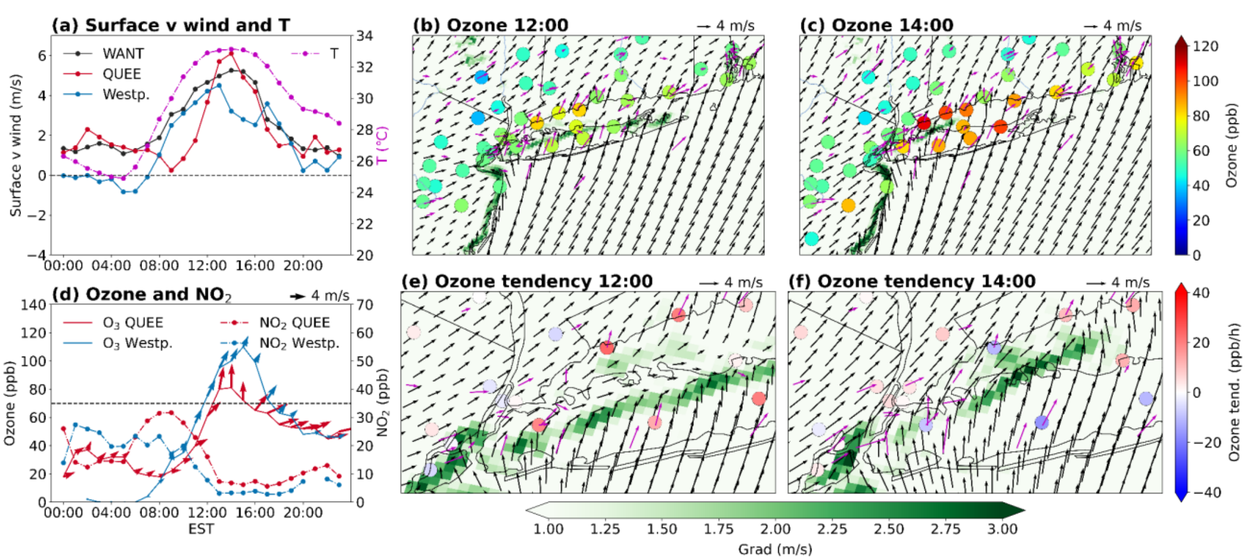

Figure 14. Same as Figure 12, but for gradual weak sea breeze onset case on Aug. 28, 2018.

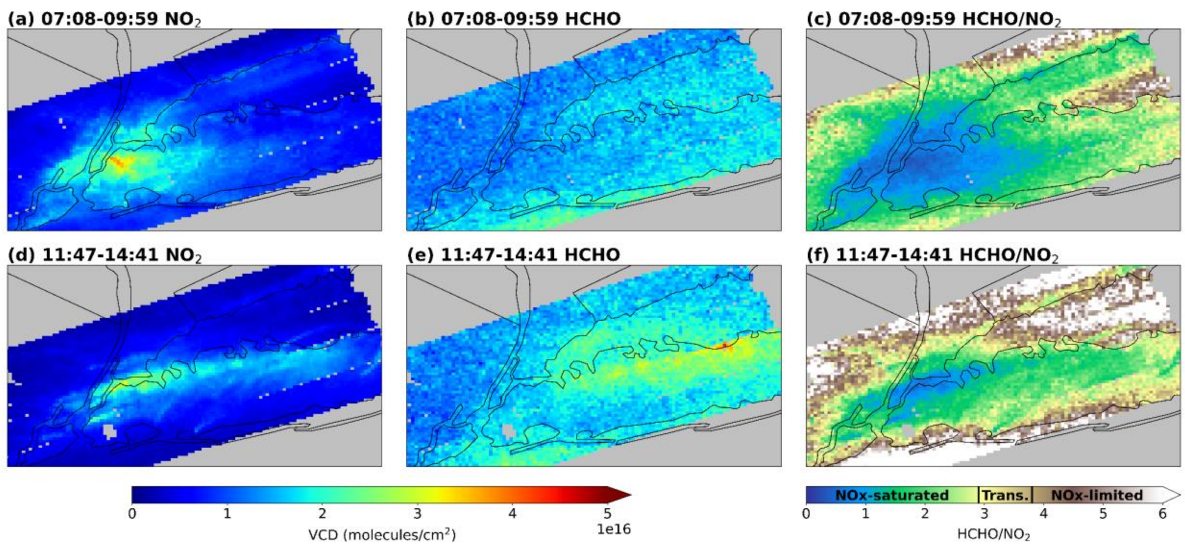

Figure 15. Same as Figure 13, but for gradual weak sea breeze onset case on Aug. 28, 2018 (data from GCAS).

4 Conclusions

This study comprehensively investigated the impacts of local circulation on coastal ozone pollution in the NY metropolitan area using three summers (2017-2019) of meteorological and chemical observations. We adopted the k-means clustering technique to cluster NYC diurnal temperature profiles and wind conditions. The meteorological conditions were grouped into three temperature clusters of hot, moderate, and cool days and four wind clusters of sea breeze, oscillation, southerly, and westerly days. It is found that specific wind patterns exhibit consistent effects on the spatial distribution of ozone regardless of temperature levels. For example, sea breeze days favor high ozone levels along the Philadelphia-NYC-LIS corridor at both hot and moderate temperatures. The most polluted days are closely associated with classic hot sea breeze days with weak large-scale flow with a regional mean DMA8 of 60.4 ppb and 8.7 sites with ozone exceedances per day on average, followed by hot westerly days with DMA8 of 53.5 ppb and 2.4 sites with ozone exceedances per day.

The spatial and temporal features in ozone time series with respect to local circulation conditions during hot summer days and how local circulations contribute to such variations are further studied. When sea breeze development in the New York Bight is delayed and its penetration into the NYC and northwestern LIS is intercepted by the dominant westerlies, DMA8 in some ozone hot spots of NYC and the south shore of CT would drop 9-10 ppb under comparable temperature levels. The average regional decrease of DMA8 for NYC and coastal CT is 6.7 and 8.3 ppb, respectively. Meanwhile, ozone build-up time in LI and eastern CT becomes hours longer, and DMA8 increases by 3.1 ppb on average because of the stationary sea breeze/westerly front along the coast. The overall probability of DMA8 exceeding the NAAQS level of 70 ppb is also dramatically decreased from 18.9% to 5.9%. Ozone exceedance is highly unlikely with marine air present in the region during hot southerly days.

Furthermore, meteorological characteristics most critical in modulating ozone exceedances in NYC and the south shore of CT during extreme hot sea breeze days are identified and analyzed with case studies during the LISTOS field campaign. As expected, ozone exceedances are very common. During these days, a relatively stronger northerly wind component (offshore) in the early morning will likely lead to an abrupt strong sea breeze onset and contribute to a lower possibility of ozone exceedances on the south shore of CT. On the contrary, a relatively stronger southerly wind component (onshore) in the early morning will favor gradual weak sea breeze development and would typically yield lower chances of ozone exceedances in NYC. Ozone level in the NYC region (Queens, NY) increases before the major sea breeze front from the Atlantic Ocean arrives in both scenarios and typically drops immediately after the sea breeze front passes by. However, ozone level continues to rise and remains at high concentrations when the further north movement of the sea breeze is hindered by a long period of convergent flow into the NYC generated by complex local circulation systems such as urban heat island. On the south coast of CT (Westport, CT), ozone is more NOx-sensitive. Ozone plateaus early from around 10:00-11:00 till late afternoon around 18:00-19:00 due to the limited NOx transported into the region and lower local emission levels in the abrupt strong sea breeze case. When abundant NOx is brought downwind into the LIS and coastal CT in the gradual weak sea breeze case, high spikes of ozone around noontime are observed, leading to much higher ozone peaks and DMA8 levels in the region.

In summary, this three-summer study comprehensively examines the impacts of local circulation on the coastal ozone problem in the NY metropolitan area. It concludes how surface ozone is impacted spatially and temporally under different temperature scenarios: all summer days, hot summer days, and extreme heat. It will serve as a reference for future case studies and provide helpful guidance for future monitor deployments or field campaigns in the region. However, due to the limited vertical observations in such a long timeframe, this study does not cover ozone vertical profiles.

Despite being extensively studied, coastal urban environments are complicated and warrant further investigations with high-resolution monitoring and modeling. In this study, only one site for each of the most polluted regions of NYC and the south coast of CT is studied due to the lack of high spatial resolution observation networks, especially those of ozone precursors. Spatially, the addition of ozone monitoring sites along the coastline of LI would benefit the understanding of the spatial extent of ozone pollution and the land/sea air interactions. As inferred from the LISTOS NO_2 and HCHO column retrievals, the current ozone monitoring network may have potentially overlooked the high ozone plume on the north shore of LI, where extreme high ozone levels are also likely in addition to the two regions studied above. Extensive field campaigns such as LISTOS are beneficial in studying atmospheric physics and chemistry in coastal urban environments and validating/developing 3-D numerical models for civil, scientific, and policy-relevant use whenever/wherever observations are not feasible.

Acknowledgements

This work is supported by the New York State Energy Research and Development Authority (NYSERDA) project (100417). We thank the support from the NYSERDA program manager, Ellen Burkhard. We also thank the Project Advisory Committee, Ruby Tian, Daniel Jacob, Praveen Amar, and Jim Szykman, for their scientific input. This work also benefits from insightful discussions with Jeffrey Freedman, Elizabeth McCabe, Chin-An Lin, Liam Sheji from Atmospheric Sciences Research Center (ASRC) and Rajesh Kumar and Stefano Alessandrini from National Center for Atmospheric Research (NCAR).

We are grateful for the data made openly available at the Environmental Protection Agency (EPA) Air Quality System (AQS, https://aqs.epa.gov/aqsweb/airdata/download_files.html), the Automated Surface Observing Systems (ASOS, https://www.ncei.noaa.gov/products/land-based-station), the National Data Buoy Center (NDBC, https://www.ndbc.noaa.gov/), the National Oceanic and Atmospheric Administration (NOAA) High-Resolution Rapid Refresh (HRRR, https://registry.opendata.aws/noaa-hrrr-pds/), and the LISTOS campaign (https://www-air.larc.nasa.gov/cgi-bin/ArcView/listos). We thank NorthEast States for Coordinated Air Use Management (NESCAUM) for coordinating LISTOS (https://www-f.nescaum.org/documents/listos). We also thank our colleagues at ASRC for providing the New

York State Mesonet (NYSM, https://www2.nysmesonet.org/) surface and Doppler lidar observations. This research is made possible by the New York State (NYS) Mesonet. Original funding for the NYS Mesonet was provided by Federal Emergency Management Agency grant FEMA-4085-DR-NY, with the continued support of the NYS Division of Homeland Security & Emergency Services; the State of New York; the Research Foundation for the State University of New York (SUNY); the University at Albany; the ASRC at the University at Albany; and the Department of Atmospheric and Environmental Sciences (DAES) at the University at Albany.

Last but not least, we would like to extend our sincere appreciation to the anonymous reviewers for their valuable time and constructive feedback, which greatly contributed to the improvement of this manuscript.

Open Research

Key scripts to cluster meteorological conditions and corresponding cluster results, as well as other supporting materials, are openly accessible under the MIT License at https://doi.org/10.5281/zenodo.10668892 (Luo & Lu, 2024).

References

Banta, R. M., Senff, C. J., Nielsen-Gammon, J., Darby, L. S., Ryerson, T. B., Alvarez, R. J., et al. (2005). A bad air day in Houston. *Bulletin of the American Meteorological Society*, *86*(5), 657–670. https://doi.org/10.1175/BAMS-86-5-657

Blaylock, B. K., Horel, J. D., & Crosman, E. T. (2017). Impact of lake breezes on summer ozone concentrations in the Salt Lake Valley. *Journal of Applied Meteorology and Climatology*, *56*(2), 353–370. https://doi.org/10.1175/JAMC-D-16-0216.1

Bornstein, R. D., & Thompson, W. T. (1981). Effects of frictionally retarded sea breeze and synoptic frontal passages on sulfur dioxide concentrations in New York City. *Journal of Applied Meteorology and Climatology*, *20*(8), 843–858. https://doi.org/10.1175/1520-0450(1981)020<0843:EOFRSB>2.0.CO;2

Brotzge, J. A., Wang, J., Thorncroft, C. D., Joseph, E., Bain, N., Bassill, N., et al. (2020). A technical overview of the New York State Mesonet Standard Network. *Journal of Atmospheric and Oceanic Technology*, *37*(10), 1827–1845. https://doi.org/10.1175/JTECH-D-19-0220.1

Caicedo, V., Rappenglueck, B., Cuchiara, G., Flynn, J., Ferrare, R., Scarino, A. J., et al. (2019). Bay breeze and sea breeze circulation impacts on the planetary boundary layer and air quality from an observed and modeled DISCOVER-AQ Texas case study. *Journal of Geophysical Research: Atmospheres*, *124*(13), 7359–7378. https://doi.org/10.1029/2019JD030523

Coates, J., Mar, K. A., Ojha, N., & Butler, T. M. (2016). The influence of temperature on ozone production under varying NO_x conditions – a modelling study. *Atmospheric Chemistry and Physics*, *16*(18), 11601–11615. https://doi.org/10.5194/acp-16-11601-2016

Couillard, M. H., Schwab, M. J., Schwab, J. J., Lu, C.-H. (Sarah), Joseph, E., Stutsrim, B., et al. (2021). Vertical profiles of ozone concentrations in the lower troposphere downwind of

New York City during LISTOS 2018–2019. *Journal of Geophysical Research: Atmospheres*, *126*(23), e2021JD035108. https://doi.org/10.1029/2021JD035108

Ding, A., Wang, T., Zhao, M., Wang, T., & Li, Z. (2004). Simulation of sea-land breezes and a discussion of their implications on the transport of air pollution during a multi-day ozone episode in the Pearl River Delta of China. *Atmospheric Environment*, *38*(39), 6737–6750. https://doi.org/10.1016/j.atmosenv.2004.09.017

Ferdiansyah, M. R., Inagaki, A., & Kanda, M. (2020). Detection of sea-breeze inland penetration in the coastal-urban region using geostationary satellite images. *Urban Climate*, *31*, 100586. https://doi.org/10.1016/j.uclim.2020.100586

Finardi, S., Agrillo, G., Baraldi, R., Calori, G., Carlucci, P., Ciccioli, P., et al. (2018). Atmospheric dynamics and ozone cycle during sea breeze in a Mediterranean complex urbanized coastal site. *Journal of Applied Meteorology and Climatology*, *57*(5), 1083–1099. https://doi.org/10.1175/JAMC-D-17-0117.1

Freitas, E. D., Rozoff, C. M., Cotton, W. R., & Dias, P. L. S. (2007). Interactions of an urban heat island and sea-breeze circulations during winter over the metropolitan area of São Paulo, Brazil. *Boundary-layer Meteorology*, 122, 43-65.

Gaza, R. S. (1998). Mesoscale meteorology and high ozone in the Northeast United States. *Journal of Applied Meteorology and Climatology*, *37*(9), 961–977. https://doi.org/10.1175/1520-0450(1998)037<0961:MMAHOI>2.0.CO;2

Guenther, A., Hewitt, C. N., Erickson, D., Fall, R., Geron, C., Graedel, T., et al. (1995). A global model of natural volatile organic compound emissions. *Journal of Geophysical Research: Atmospheres*, *100*(D5), 8873–8892. https://doi.org/10.1029/94JD02950

Haman, C. L., Couzo, E., Flynn, J. H., Vizuete, W., Heffron, B., & Lefer, B. L. (2014). Relationship between boundary layer heights and growth rates with ground-level ozone in Houston, Texas. Journal of Geophysical Research: Atmospheres, 119(10), 6230-6245. https://doi.org/10.1002/2013JD020473

Han, Z. S., González-Cruz, J. E., Liu, H. N., Melecio-Vázquez, D., Gamarro, H., Wu, Y. H., et al. (2022). Observed sea breeze life cycle in and around NYC: impacts on UHI and ozone patterns. *Urban Climate*, *42*, 101109. https://doi.org/10.1016/j.uclim.2022.101109

Hu, T., Wang, Y., & Wu, D. (2022). The interaction of an urban heat island with a sea breeze front during moist convection over Tianjin, China. *Weather*, 77(7), 238-247.

Jin, X., Fiore, A., Boersma, K. F., Smedt, I. D., & Valin, L. (2020). Inferring changes in summertime surface ozone–NOx–VOC chemistry over U.S. urban areas from two decades of satellite and ground-based observations. *Environmental Science & Technology*, *54*(11), 6518–6529. https://doi.org/10.1021/acs.est.9b07785

Khiem, M., Ooka, R., Huang, H., Hayami, H., Yoshikado, H., & Kawamoto, Y. (2010). Analysis of the relationship between changes in meteorological conditions and the variation in summer ozone levels over the Central Kanto area. *Advances in Meteorology*, *2010*, e349248. https://doi.org/10.1155/2010/349248

Li, W., Wang, Y., Bernier, C., & Estes, M. (2020). Identification of sea breeze recirculation and its effects on ozone in Houston, TX, during DISCOVER-AQ 2013. *Journal of Geophysical Research: Atmospheres*, *125*(22), e2020JD033165. https://doi.org/10.1029/2020JD033165

Liu, J., Song, X., Long, W., Fu, Y., Yun, L., & Zhang, M. (2022). Structure analysis of the sea breeze based on Doppler lidar and its impact on pollutants. *Remote Sensing*, *14*(2), 324. https://doi.org/10.3390/rs14020324

Luo, H., & Lu, C. H. (2024). LocalCirculation_CoastalOzone_NewYorkMetro: Luo_JRG_v0 (Version 0) [Dataset]. *Zenodo*. https://doi.org/10.5281/zenodo.10668892

Macqueen, J. (1967). Some methods for classification and analysis of multivariate observations. *Proc. Fifth Berkeley Symp. Math. Statistics and Probability, 1967*, *1*, 281–297.

McCabe, E. J., & Freedman, J. M. (2023). Development of an objective methodology for identifying the sea breeze circulation and associated low-level jet in the New York Bight. *Weather and Forecasting*, 38(4), 571-589. https://doi.org/10.1175/WAF-D-22-0119.1

Ngan, F., & Byun, D. (2011). Classification of weather patterns and associated trajectories of high-ozone episodes in the Houston–Galveston–Brazoria area during the 2005/06 TexAQS-II. *Journal of Applied Meteorology and Climatology*, *50*(3), 485–499. https://doi.org/10.1175/2010JAMC2483.1

Novak, D. R., & Colle, B. A. (2006). Observations of multiple sea breeze boundaries during an unseasonably warm day in metropolitan New York City. *Bulletin of the American Meteorological Society*, *87*(2), 169–174. https://doi.org/10.1175/BAMS-87-2-169

Oh, I.-B., Kim, Y.-K., Lee, H. woon, & Kim, C.-H. (2006). An observational and numerical study of the effects of the late sea breeze on ozone distributions in the Busan metropolitan area, Korea. *Atmospheric Environment*, *40*(7), 1284–1298. https://doi.org/10.1016/j.atmosenv.2005.10.049

Olszyna, K. J., Luria, M., & Meagher, J. F. (1997). The correlation of temperature and rural ozone levels in southeastern U.S.A. *Atmospheric Environment*, *31*(18), 3011–3022. https://doi.org/10.1016/S1352-2310(97)00097-6

Ortiz, L. E., González, J. E., Horton, R., Lin, W., Wu, W., Ramamurthy, P., et al. (2019). High-resolution projections of extreme heat in New York City. *International Journal of Climatology*, *39*(12), 4721–4735. https://doi.org/10.1002/joc.6102

Papanastasiou, D. K., & Melas, D. (2009). Climatology and impact on air quality of sea breeze in an urban coastal environment. *International Journal of Climatology*, *29*(2), 305–315. https://doi.org/10.1002/joc.1707

Pedregosa, F., Varoquaux, G., Gramfort, A., Michel, V., Thirion, B., Grisel, O., ... & Duchesnay, É. (2011). Scikit-learn: Machine learning in Python. *Journal of Machine Learning Research*, 12, 2825-2830.

Porter, W. C., & Heald, C. L. (2019). The mechanisms and meteorological drivers of the summertime ozone–temperature relationship. *Atmospheric Chemistry and Physics*, *19*(21), 13367–13381. https://doi.org/10.5194/acp-19-13367-2019

Shen, L., Zhao, C., Ma, Z., Li, Z., Li, J., & Wang, K. (2019). Observed decrease of summer sea-land breeze in Shanghai from 1994 to 2014 and its association with urbanization. *Atmospheric Research*, *227*, 198–209. https://doi.org/10.1016/j.atmosres.2019.05.007

Shrestha, B., Brotzge, J. A., Wang, J., Bain, N., Thorncroft, C. D., Joseph, E., et al. (2021). Overview and applications of the New York State Mesonet Profiler Network. *Journal of Applied Meteorology and Climatology*, *60*(11), 1591–1611. https://doi.org/10.1175/JAMC-D-21-0104.1

Tao, M., Fiore, A. M., Jin, X., Schiferl, L. D., Commane, R., Judd, L. M., et al. (2022). Investigating changes in ozone formation chemistry during summertime pollution events over the Northeastern United States. *Environmental Science & Technology*, 56(22), 15312-15327. https://doi.org/10.1021/acs.est.2c02972

Torres-Vazquez, A., Pleim, J., Gilliam, R., & Pouliot, G. (2022). Performance evaluation of the meteorology and air quality conditions from multiscale WRF-CMAQ simulations for the

Long Island Sound Tropospheric Ozone Study (LISTOS). *Journal of Geophysical Research: Atmospheres*, *127*(5), e2021JD035890. https://doi.org/10.1029/2021JD035890

Ulpiani, G. (2021). On the linkage between urban heat island and urban pollution island: three-decade literature review towards a conceptual framework. *Science of The Total Environment*, *751*, 141727. https://doi.org/10.1016/j.scitotenv.2020.141727

US EPA (2018, August 23). Green book 8-hour ozone (2015) area information [Data and Tools]. Retrieved November 13, 2022, from https://www.epa.gov/green-book/green-book-8-hour-ozone-2015-area-information

Xu, J., Huang, X., Wang, N., Li, Y., & Ding, A. (2021). Understanding ozone pollution in the Yangtze River Delta of eastern China from the perspective of diurnal cycles. *Science of The Total Environment*, *752*, 141928. https://doi.org/10.1016/j.scitotenv.2020.141928

Zhang, C., Jiang, Z., Liu, M., Dong, Y., & Li, J. (2023). Relationship between summer time near-surface ozone concentration and planetary boundary layer height in Beijing. *Atmospheric Research*, 106892. https://doi.org/10.1016/j.atmosres.2023.106892

Zhang, J., Ninneman, M., Joseph, E., Schwab, M. J., Shrestha, B., & Schwab, J. J. (2020). Mobile laboratory measurements of high surface ozone levels and spatial heterogeneity during LISTOS 2018: evidence for sea breeze influence. *Journal of Geophysical Research: Atmospheres*, *125*(11), e2019JD031961. https://doi.org/10.1029/2019JD031961

Zhang, J., Catena, A., Shrestha, B., Freedman, J., McCabe, E., Schwab, M. J., et al. (2022). Unraveling the interaction of urban emission plumes and marine breezes involved in the formation of summertime coastal high ozone on Long Island. *Environmental Science: Atmospheres*, *2*(6), 1438–1449. https://doi.org/10.1039/D2EA00061J

Zhang, R., Lei, W., Tie, X., & Hess, P. (2004). Industrial emissions cause extreme urban ozone diurnal variability. *Proceedings of the National Academy of Sciences*, *101*(17), 6346–6350. https://doi.org/10.1073/pnas.0401484101

Figure 1.

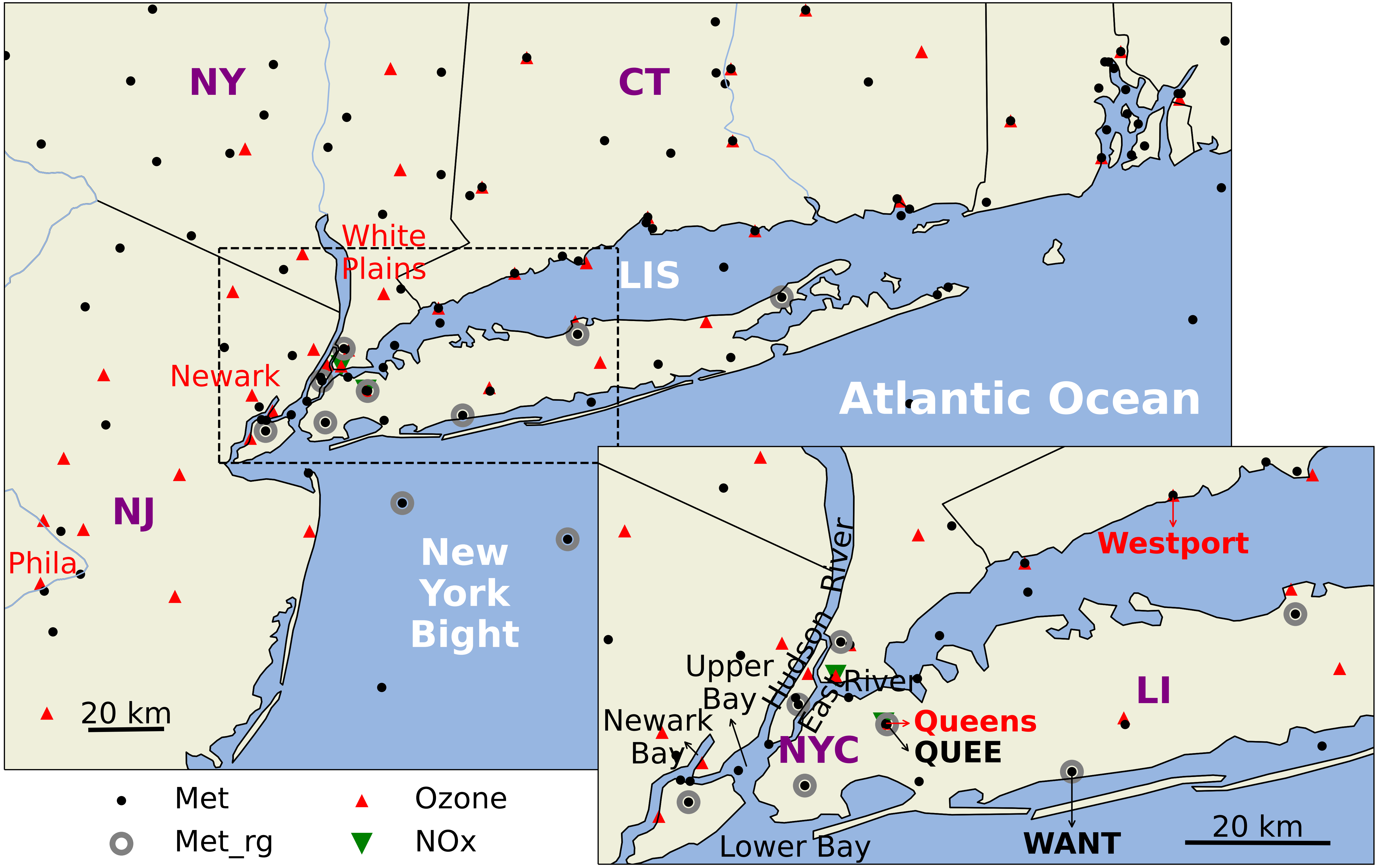
NY
CT
NJ
White Plains
Newark
Phila
LIS
Atlantic Ocean
New York Bight
20 km
Met
Met_rg
Ozone
NOx
Westport
Hudson River
East River
Upper Bay
Newark Bay
NYC
Queens
QUEE
LI
Lower Bay
WANT
20 km

Figure 2.

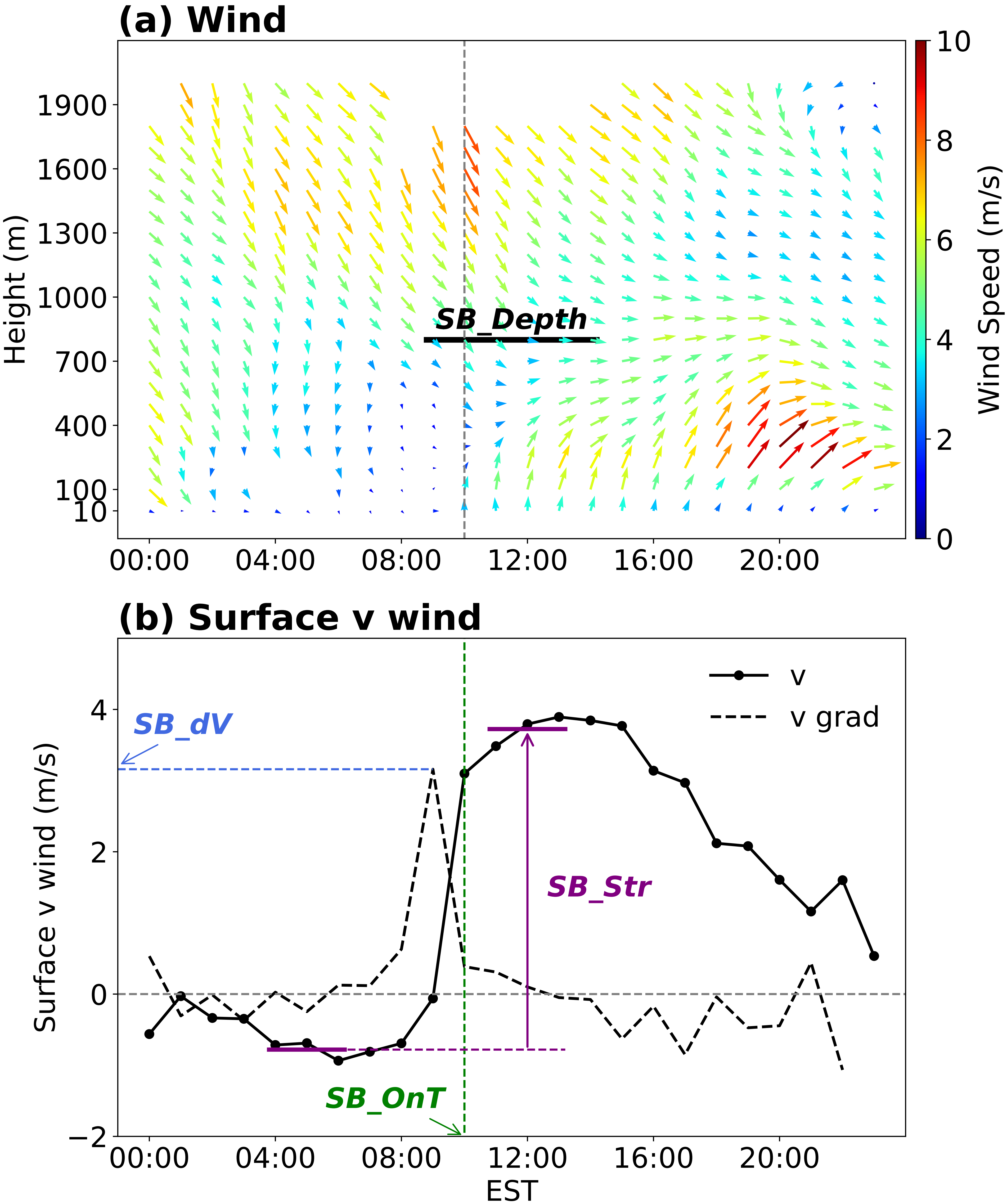

(a) Wind
Height (m)
Wind Speed (m/s)
SB_Depth
(b) Surface v wind
Surface v wind (m/s)
SB_dV
SB_Str
SB_OnT
v
v grad
EST

Figure 3.

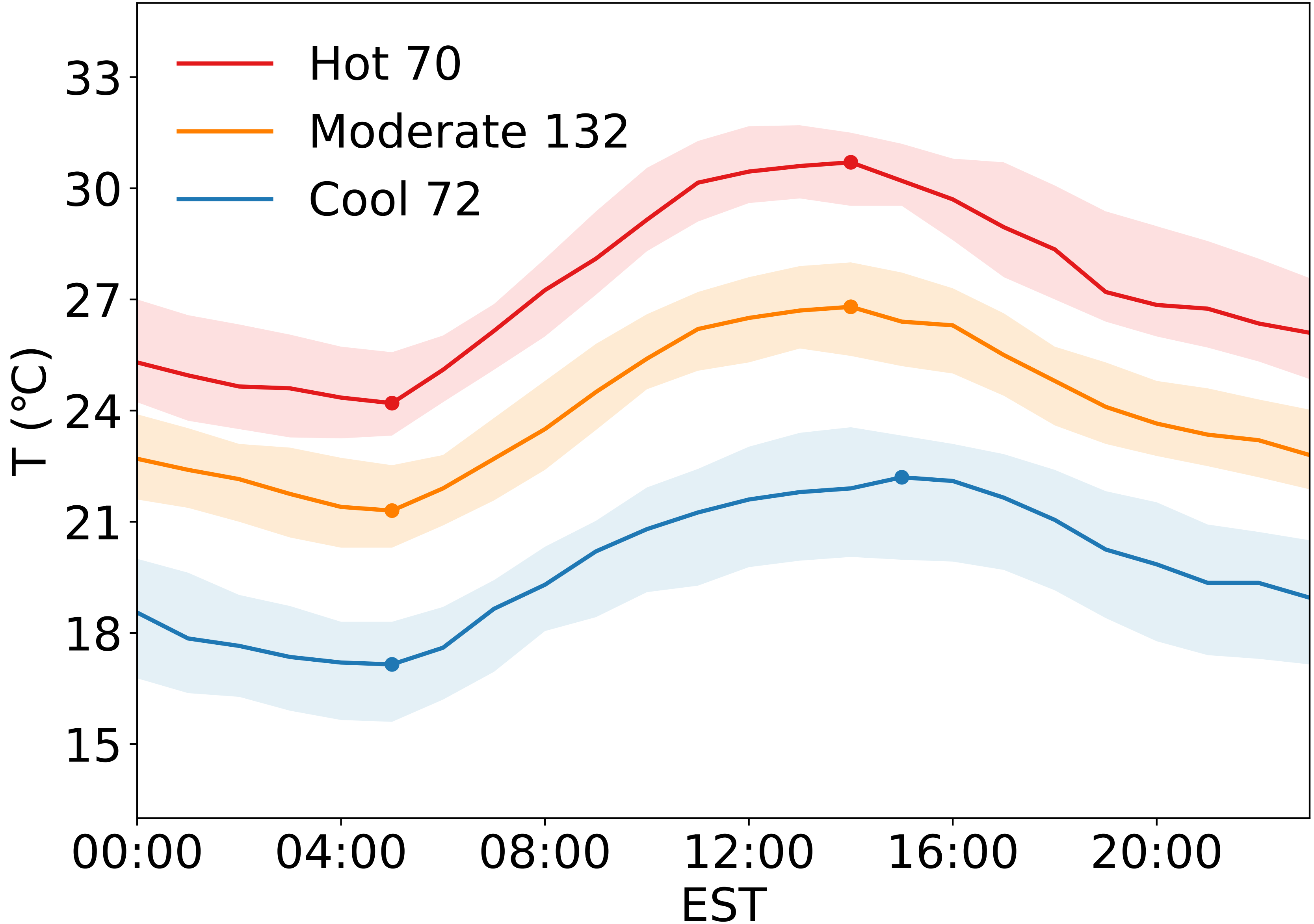
Hot 70
Moderate 132
Cool 72
T (°C)
33
30
27
24
21
18
15
00:00
04:00
08:00
12:00
16:00
20:00
EST

Figure 4.

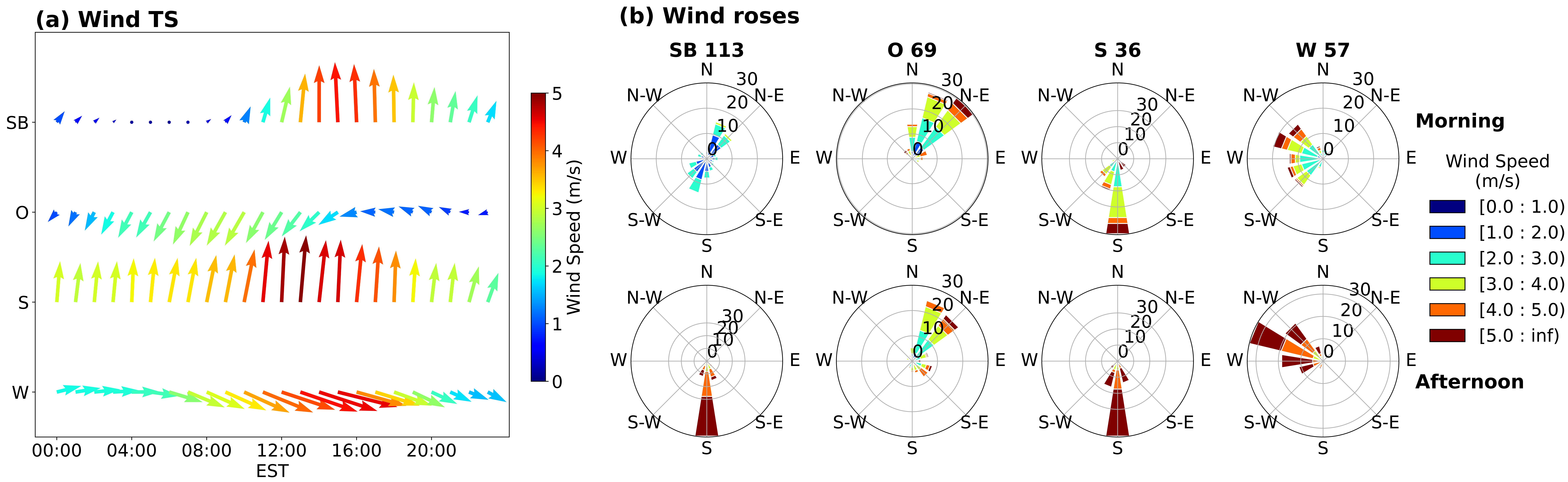
(a) Wind TS
SB
O
S
W
00:00
04:00
08:00
12:00
16:00
20:00
EST
Wind Speed (m/s)
0
1
2
3
4
5
(b) Wind roses
SB 113
O 69
S 36
W 57
N
N-E
E
S-E
S
S-W
W
N-W
0
10
20
30
Morning
Afternoon
Wind Speed (m/s)
[0.0 : 1.0)
[1.0 : 2.0)
[2.0 : 3.0)
[3.0 : 4.0)
[4.0 : 5.0)
[5.0 : inf)

Figure 5.

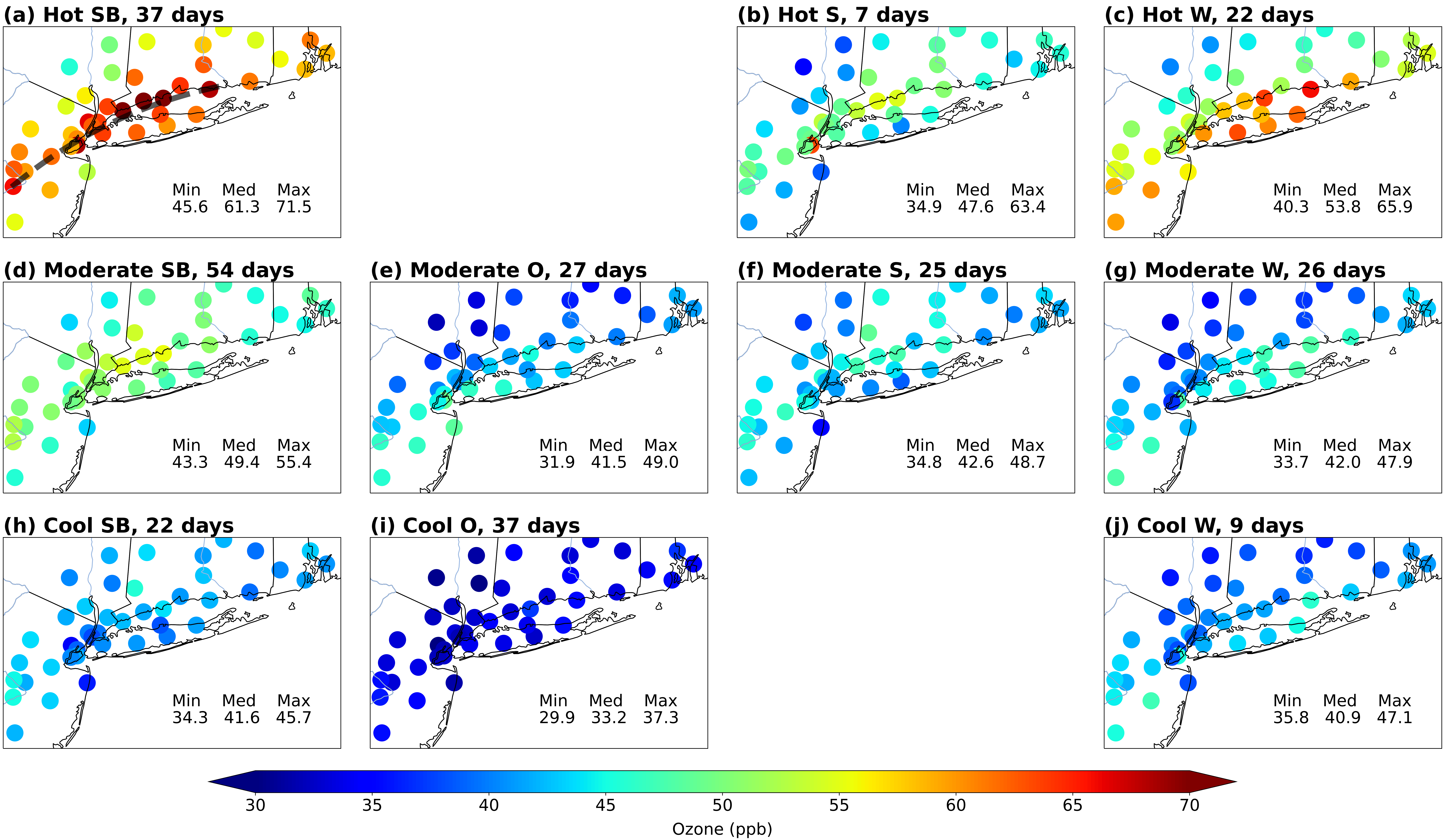

(a) Hot SB, 37 days
Min Med Max
45.6 61.3 71.5
(b) Hot S, 7 days
Min Med Max
34.9 47.6 63.4
(c) Hot W, 22 days
Min Med Max
40.3 53.8 65.9
(d) Moderate SB, 54 days
Min Med Max
43.3 49.4 55.4
(e) Moderate O, 27 days
Min Med Max
31.9 41.5 49.0
(f) Moderate S, 25 days
Min Med Max
34.8 42.6 48.7
(g) Moderate W, 26 days
Min Med Max
33.7 42.0 47.9
(h) Cool SB, 22 days
Min Med Max
34.3 41.6 45.7
(i) Cool O, 37 days
Min Med Max
29.9 33.2 37.3
(j) Cool W, 9 days
Min Med Max
35.8 40.9 47.1
30 35 40 45 50 55 60 65 70
Ozone (ppb)

Figure 6.

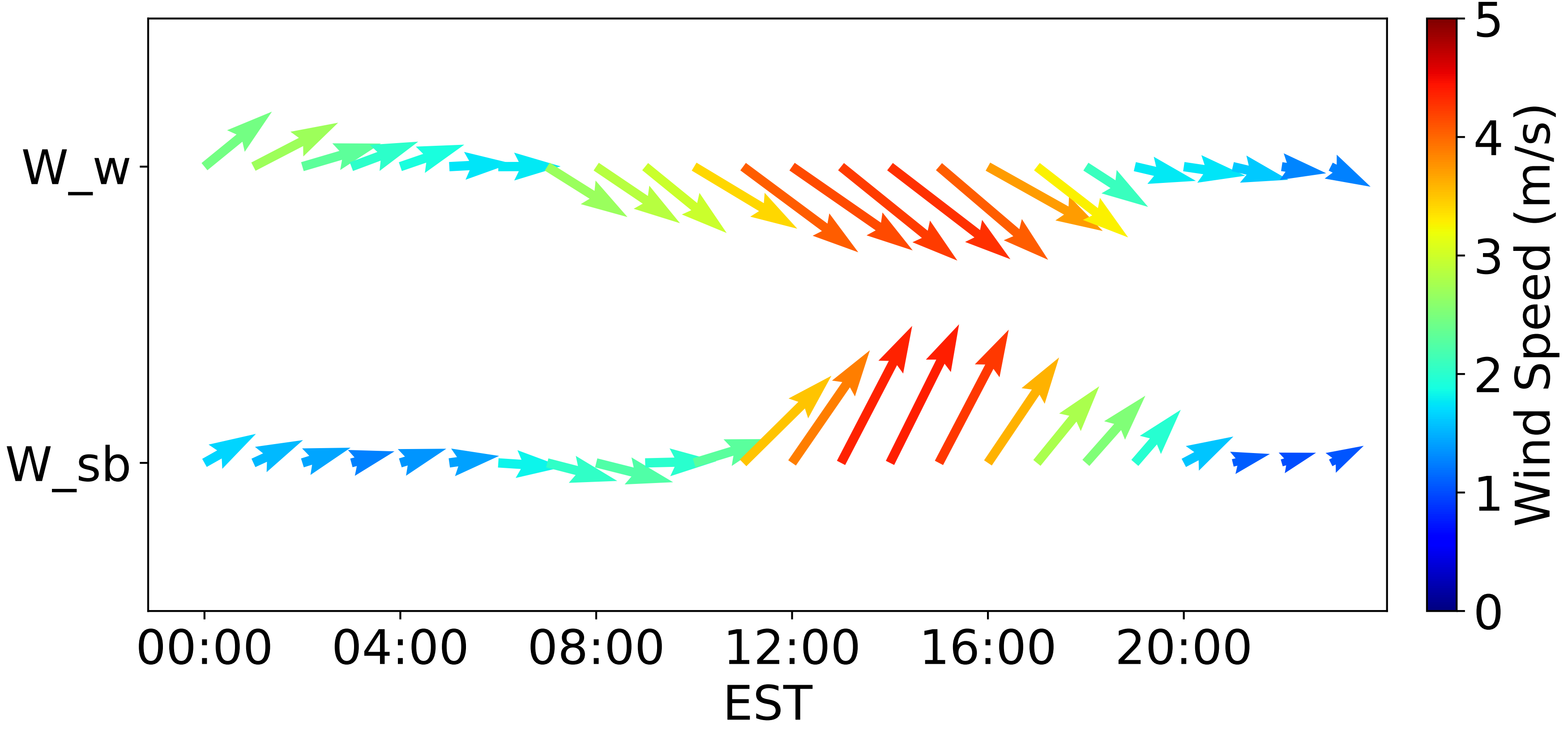

W_w
W_sb
00:00
04:00
08:00
12:00
16:00
20:00
EST
Wind Speed (m/s)
0
1
2
3
4
5

Figure 7.

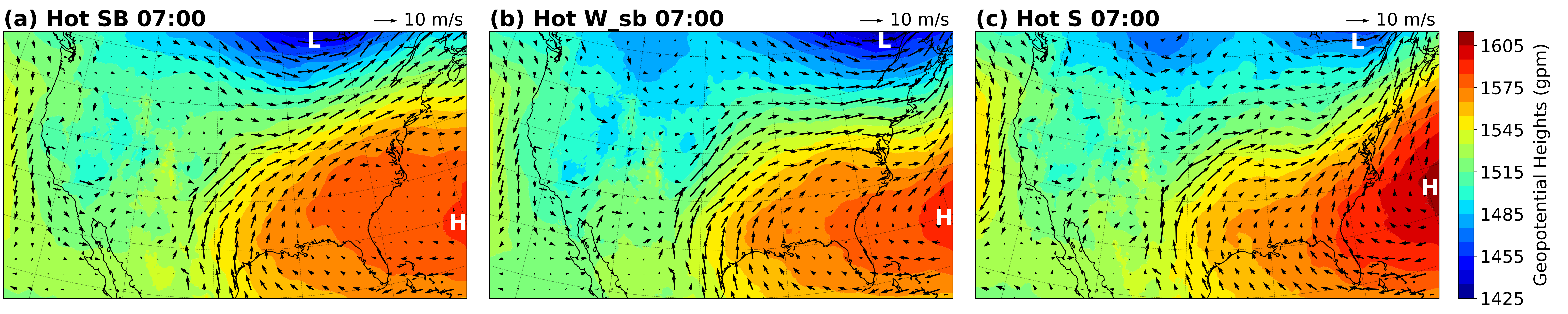
(a) Hot SB 07:00
10 m/s
L
H
(b) Hot W_sb 07:00
10 m/s
L
H
(c) Hot S 07:00
10 m/s
L
H
Geopotential Heights (gpm)
1605
1575
1545
1515
1485
1455
1425

Figure 8.

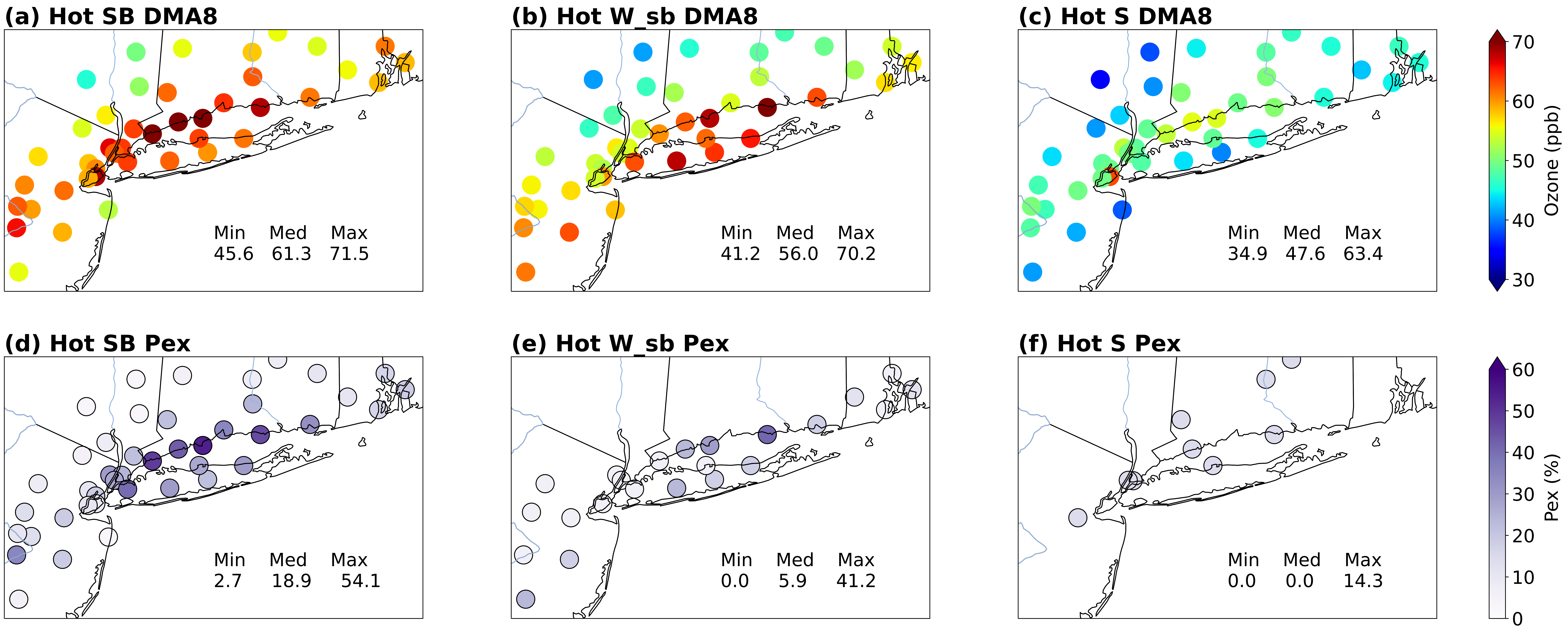
(a) Hot SB DMA8
Min 45.6
Med 61.3
Max 71.5
(b) Hot W_sb DMA8
Min 41.2
Med 56.0
Max 70.2
(c) Hot S DMA8
Min 34.9
Med 47.6
Max 63.4
Ozone (ppb)
30
40
50
60
70
(d) Hot SB Pex
Min 2.7
Med 18.9
Max 54.1
(e) Hot W_sb Pex
Min 0.0
Med 5.9
Max 41.2
(f) Hot S Pex
Min 0.0
Med 0.0
Max 14.3
Pex (%)
0
10
20
30
40
50
60

Figure 9.

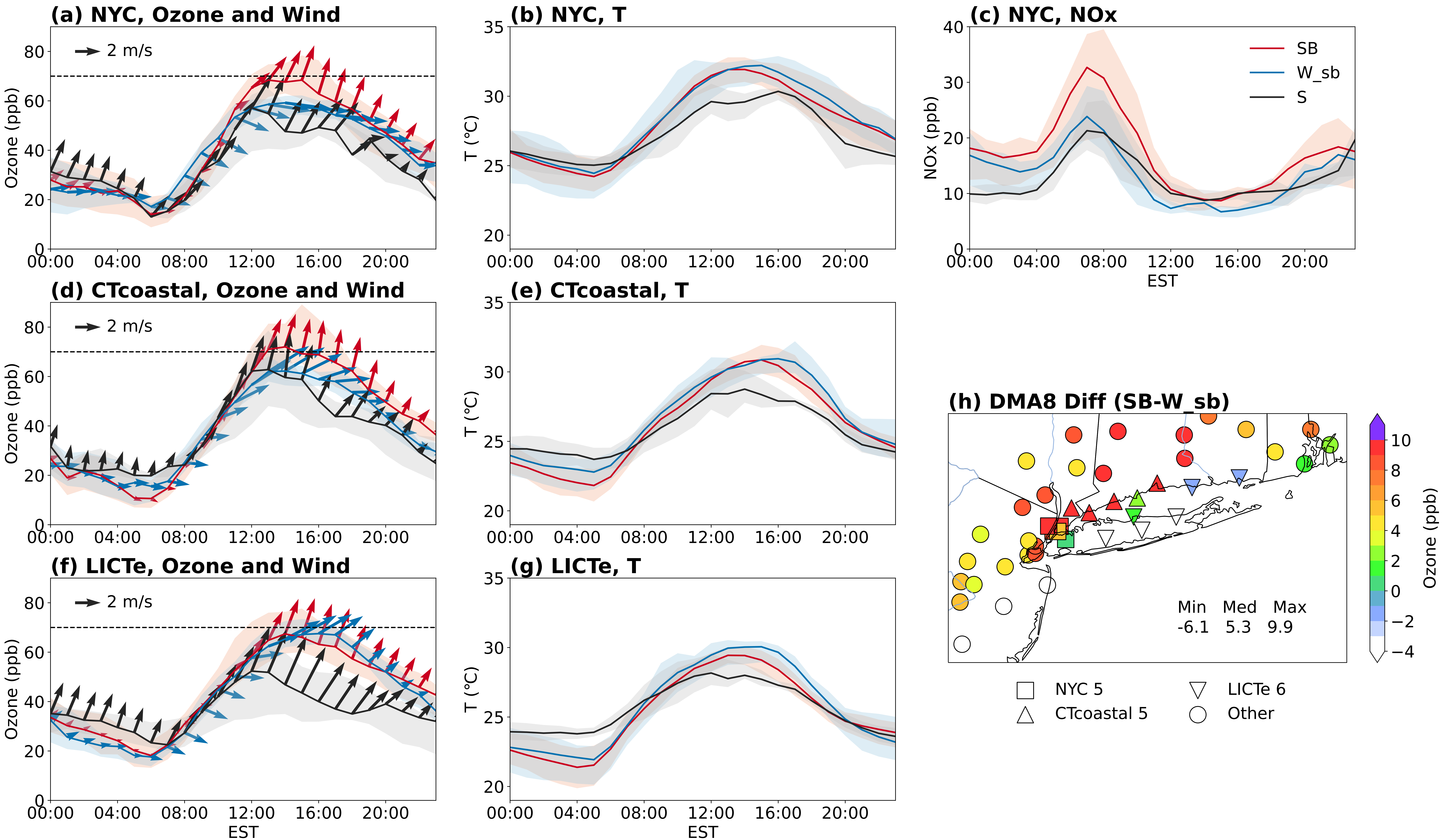

(a) NYC, Ozone and Wind
(b) NYC, T
(c) NYC, NOx
(d) CTcoastal, Ozone and Wind
(e) CTcoastal, T
(f) LICTe, Ozone and Wind
(g) LICTe, T
(h) DMA8 Diff (SB-W_sb)
2 m/s
Ozone (ppb)
T (°C)
NOx (ppb)
EST
SB
W_sb
S
Min Med Max
-6.1 5.3 9.9
NYC 5
CTcoastal 5
LICTe 6
Other

Figure 10.

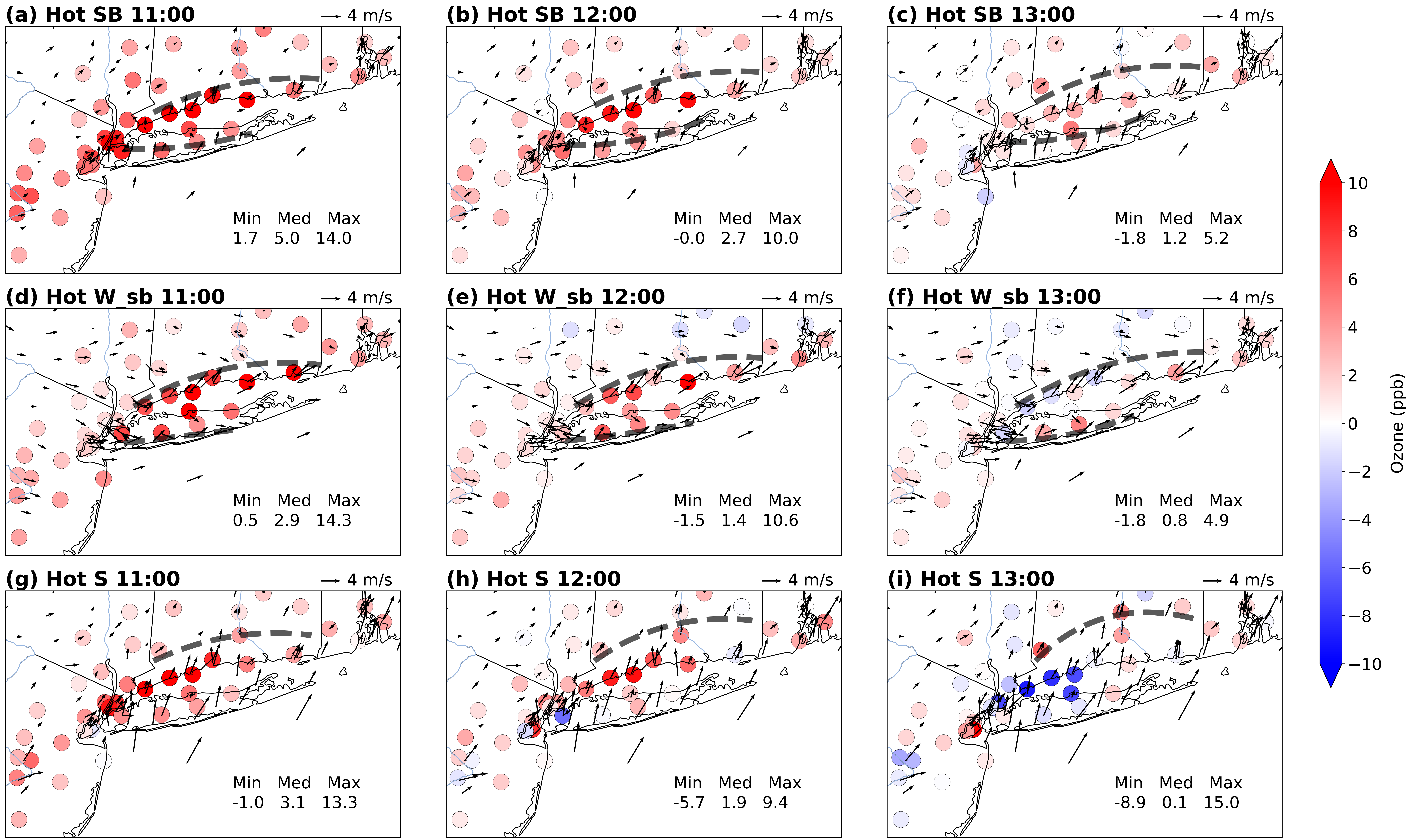

(a) Hot SB 11:00
4 m/s
Min Med Max
1.7 5.0 14.0
(b) Hot SB 12:00
4 m/s
Min Med Max
-0.0 2.7 10.0
(c) Hot SB 13:00
4 m/s
Min Med Max
-1.8 1.2 5.2
(d) Hot W_sb 11:00
4 m/s
Min Med Max
0.5 2.9 14.3
(e) Hot W_sb 12:00
4 m/s
Min Med Max
-1.5 1.4 10.6
(f) Hot W_sb 13:00
4 m/s
Min Med Max
-1.8 0.8 4.9
(g) Hot S 11:00
4 m/s
Min Med Max
-1.0 3.1 13.3
(h) Hot S 12:00
4 m/s
Min Med Max
-5.7 1.9 9.4
(i) Hot S 13:00
4 m/s
Min Med Max
-8.9 0.1 15.0
Ozone (ppb)
10
8
6
4
2
0
−2
−4
−6
−8
−10

Figure11.

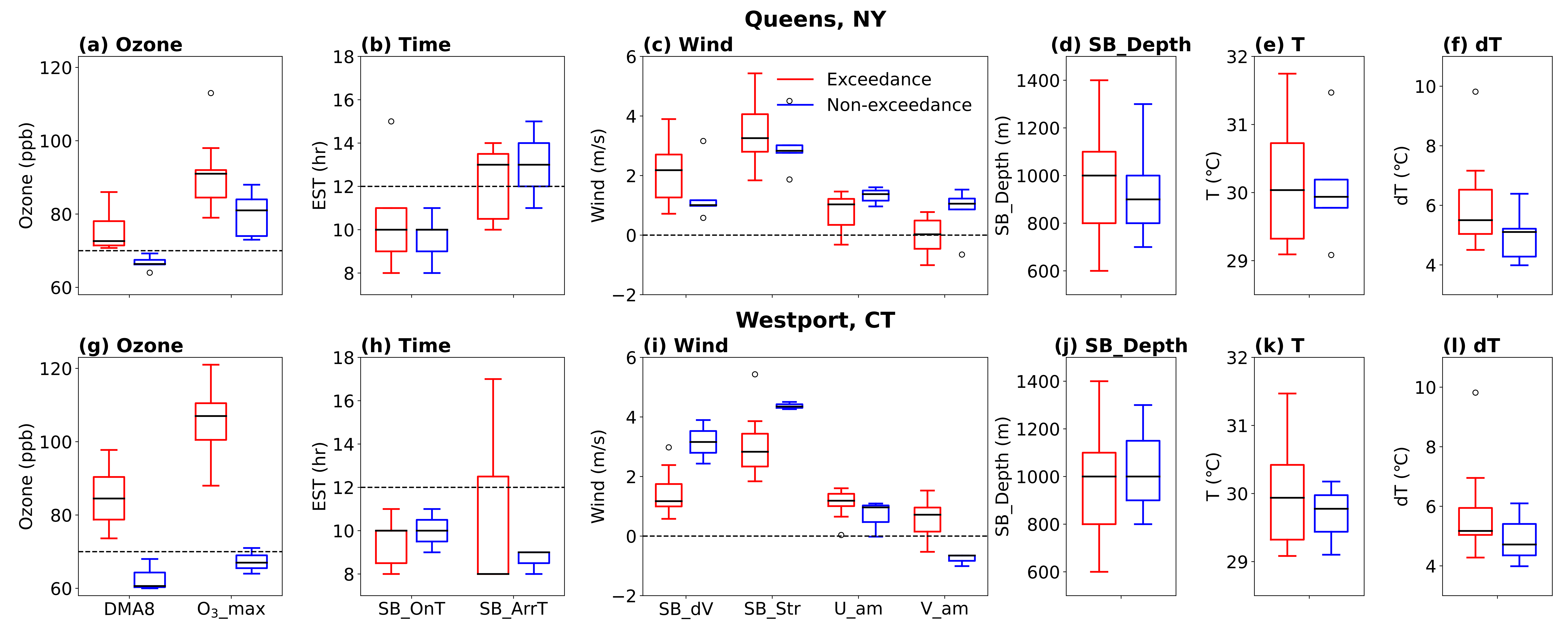

Queens, NY
(a) Ozone
(b) Time
(c) Wind
(d) SB_Depth
(e) T
(f) dT
Exceedance
Non-exceedance
Ozone (ppb)
EST (hr)
Wind (m/s)
SB_Depth (m)
T (°C)
dT (°C)
Westport, CT
(g) Ozone
(h) Time
(i) Wind
(j) SB_Depth
(k) T
(l) dT
DMA8
O_3_max
SB_OnT
SB_ArrT
SB_dV
SB_Str
U_am
V_am

Figure 12.

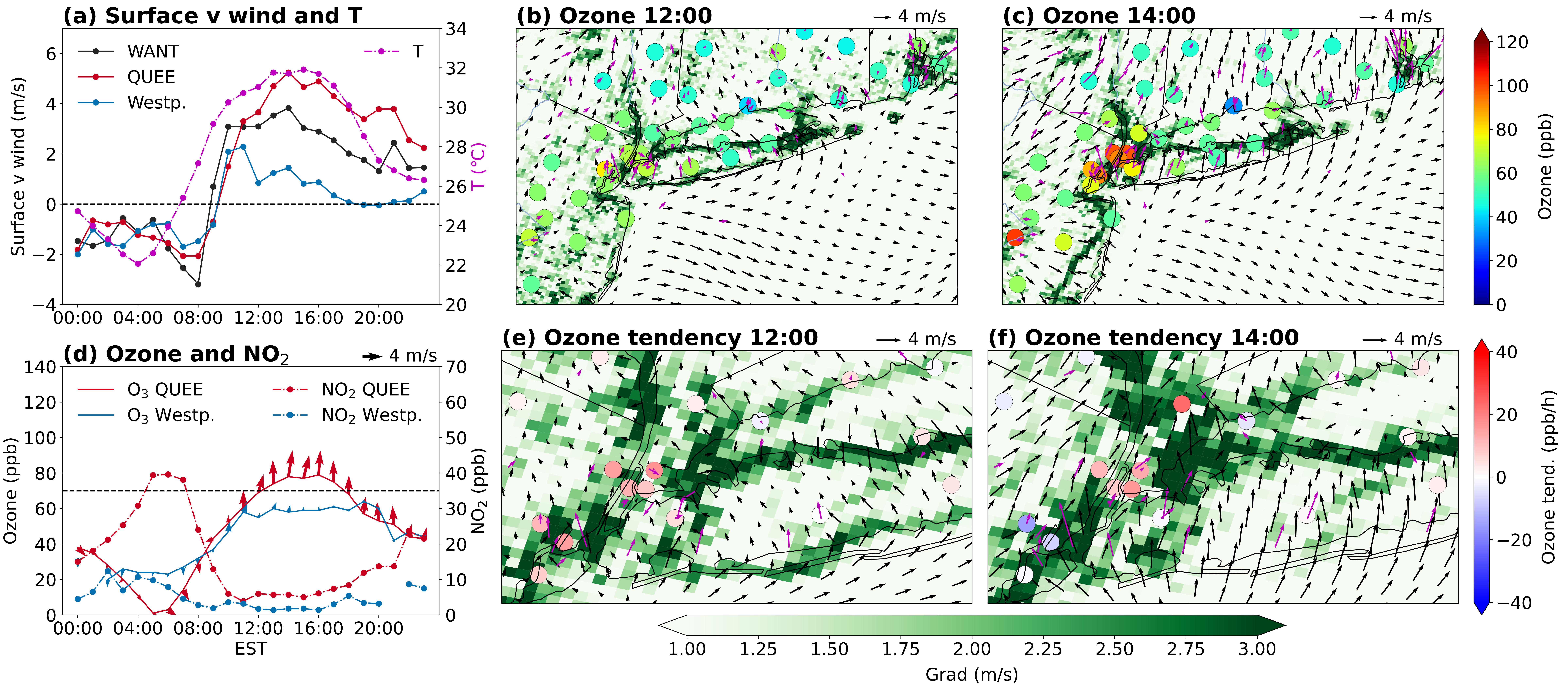
(a) Surface v wind and T
WANT
QUEE
Westp.
T
Surface v wind (m/s)
T (°C)
00:00 04:00 08:00 12:00 16:00 20:00
(b) Ozone 12:00
4 m/s
(c) Ozone 14:00
4 m/s
Ozone (ppb)
(d) Ozone and NO_2
4 m/s
O_3 QUEE
O_3 Westp.
NO_2 QUEE
NO_2 Westp.
Ozone (ppb)
NO_2 (ppb)
EST
(e) Ozone tendency 12:00
4 m/s
(f) Ozone tendency 14:00
4 m/s
Ozone tend. (ppb/h)
Grad (m/s)

Figure 13.

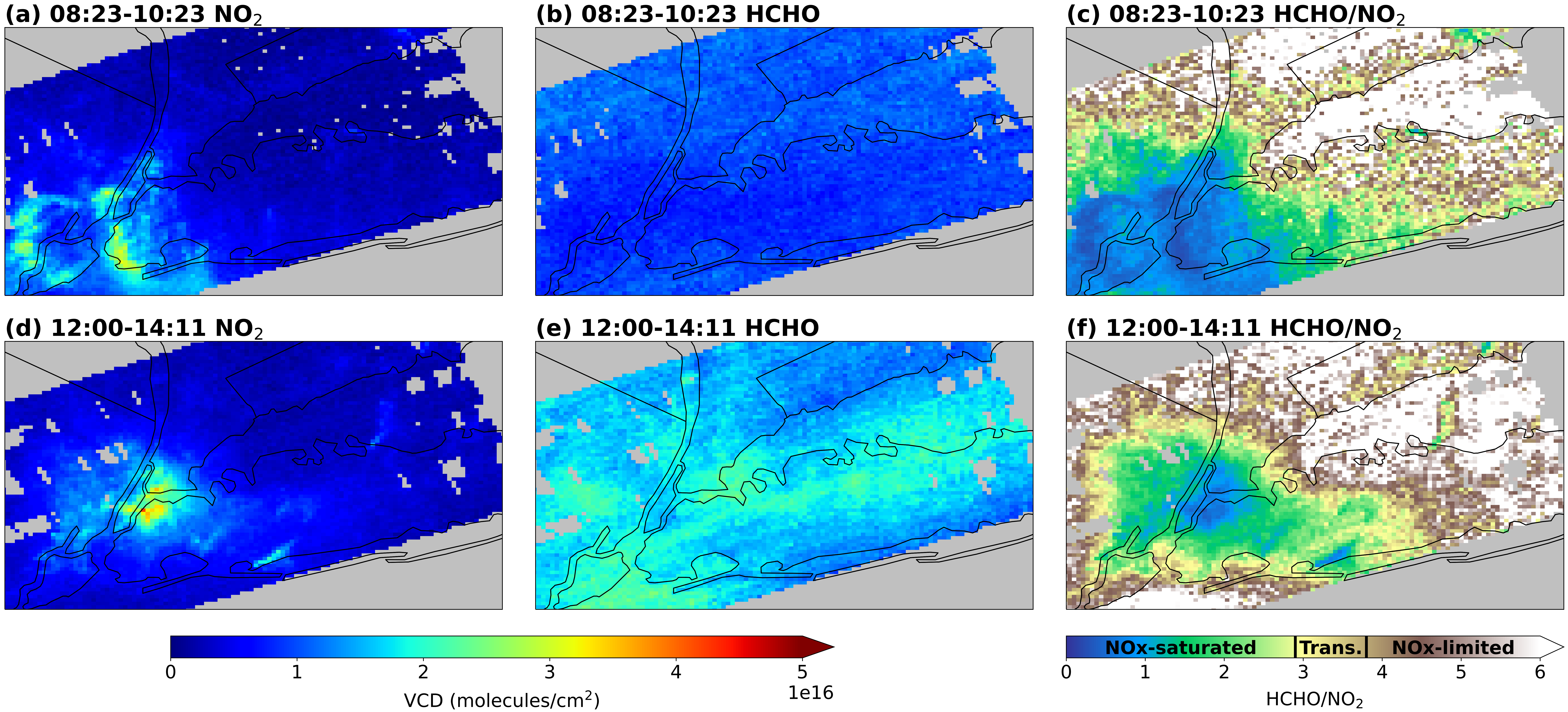

(a) 08:23-10:23 NO2
(b) 08:23-10:23 HCHO
(c) 08:23-10:23 HCHO/NO2
(d) 12:00-14:11 NO2
(e) 12:00-14:11 HCHO
(f) 12:00-14:11 HCHO/NO2
0 1 2 3 4 5
1e16
VCD (molecules/cm2)
NOx-saturated
Trans.
NOx-limited
0 1 2 3 4 5 6
HCHO/NO2

Figure 14.

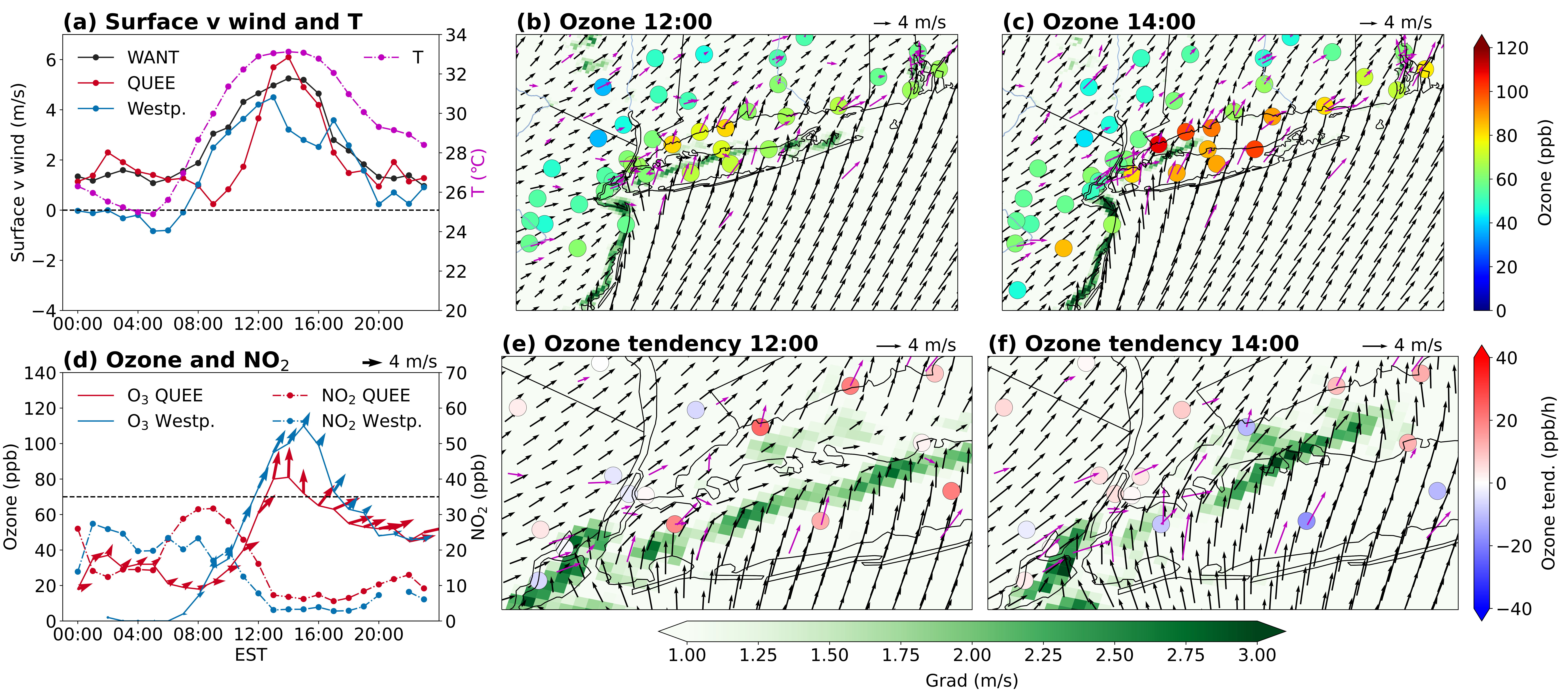

(a) Surface v wind and T
WANT
QUEE
Westp.
T
Surface v wind (m/s)
T (°C)
(b) Ozone 12:00
4 m/s
(c) Ozone 14:00
4 m/s
Ozone (ppb)
(d) Ozone and NO2
4 m/s
O3 QUEE
O3 Westp.
NO2 QUEE
NO2 Westp.
Ozone (ppb)
NO2 (ppb)
EST
(e) Ozone tendency 12:00
4 m/s
(f) Ozone tendency 14:00
4 m/s
Ozone tend. (ppb/h)
Grad (m/s)

Figure 15.

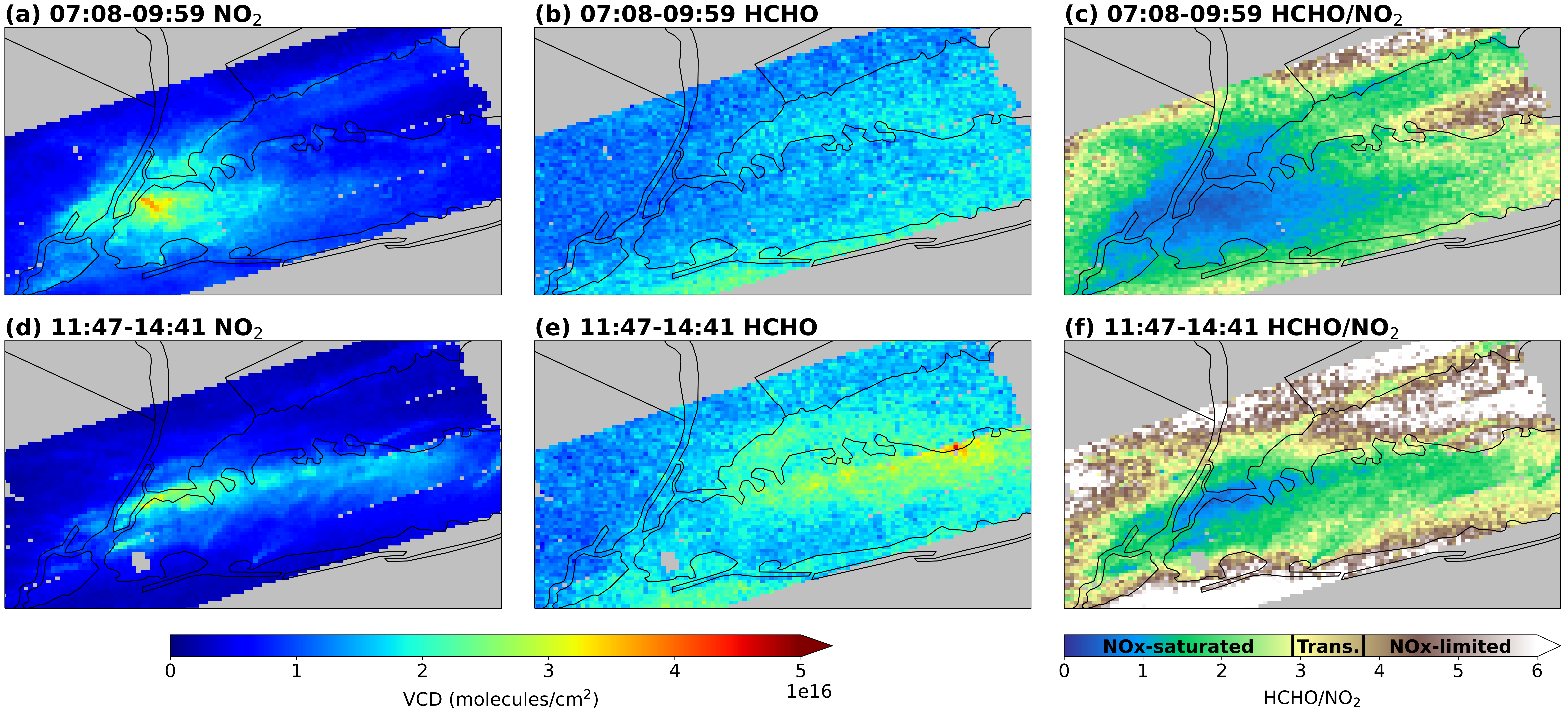
(a) 07:08-09:59 NO$_2$
(b) 07:08-09:59 HCHO
(c) 07:08-09:59 HCHO/NO$_2$
(d) 11:47-14:41 NO$_2$
(e) 11:47-14:41 HCHO
(f) 11:47-14:41 HCHO/NO$_2$
0
1
2
3
4
5
1e16
VCD (molecules/cm^2)
NOx-saturated
Trans.
NOx-limited
0
1
2
3
4
5
6
HCHO/NO$_2$